AD-A152 143 INVESTIGATION OF BASIC CHARACTERISTICS OF LASER HEATING IN THERMOLUMINESC..(U) WASHINGTON STATE UNIV PULLMAN DEPT OF PHYSICS P F BRAUNLICH 15 MAR 85 1/1

UNCLASSIFIED N00014-82-K-0529 F/G 20/5 NL

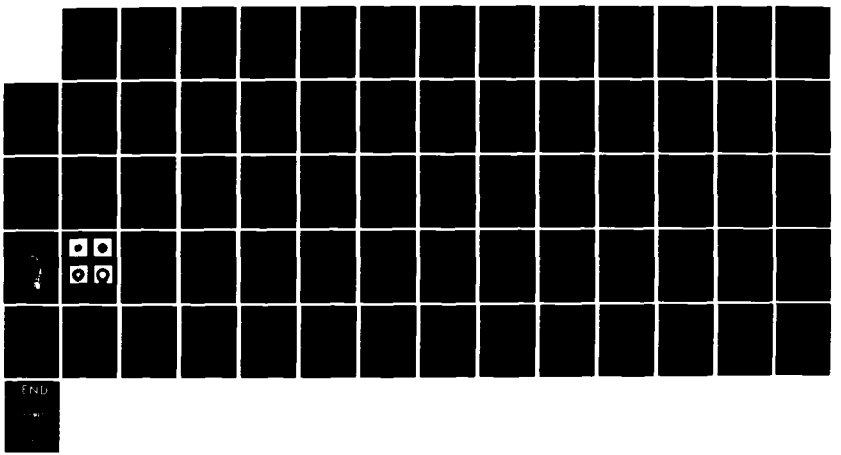

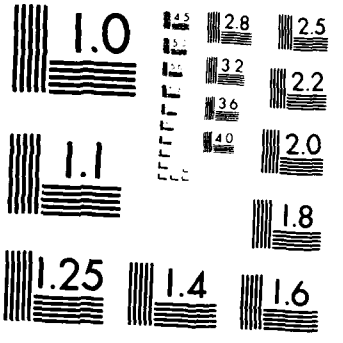

(4)

SECURITY CLASSIFICATION OF THIS PAGE (When Data Entered)

REPORT DOCUMENTATION PAGE

READ INSTRUCTIONS BEFORE COMPLETING FORM

1. REPORT NUMBER
2. GOVT ACCESSION NO.
3. RECIPIENT'S CATALOG NUMBER

4. TITLE (and Subtitle)
Investigation of Basic Characteristics of Laser Heating in Thermoluminescence and of Laser-Stimulated Luminescence

5. TYPE OF REPORT & PERIOD COVERED
Annual Summary Report
7/15/84 – 7/14/85

6. PERFORMING ORG. REPORT NUMBER

7. AUTHOR(s)
P.I. Peter F. Braumlich

8. CONTRACT OR GRANT NUMBER(s)
ONRN00014-82-K-0529

9. PERFORMING ORGANIZATION NAME AND ADDRESS
Department of Physics
Washington State University
Pullman, WA 99164-2814

10. PROGRAM ELEMENT, PROJECT, TASK AREA & WORK UNIT NUMBERS
Task Area: RR011-07-01
Work Unit: NR395-079
Program Element: 61153N

11. CONTROLLING OFFICE NAME AND ADDRESS
Office of Naval Research
800 N. Quincy Street
Arlington, VA 22217

12. REPORT DATE
3/15/85

13. NUMBER OF PAGES
Unclassified

14. MONITORING AGENCY NAME & ADDRESS(if different from Controlling Office)
Office of Naval Research, Res. Representative
University District Bldg., Room 422
1107 N.E. 45th Street
Seattle, WA 98195

15. SECURITY CLASS. (of this report)

15a. DECLASSIFICATION/DOWNGRADING SCHEDULE

16. DISTRIBUTION STATEMENT (of this Report)
Approved for public release; distribution unlimited

17. DISTRIBUTION STATEMENT (of the abstract entered in Block 20, if different from Report)

DTIC ELECTE S APR 8 1985 D B

18. SUPPLEMENTARY NOTES

19. KEY WORDS (Continue on reverse side if necessary and identify by block number)
Thermoluminescence, Thermoluminescence Dosimetry, Laser Heating, Heat Transfer, Gaussian Beam

20. ABSTRACT (Continue on reverse side if necessary and identify by block number)

Experimental and computational methods are presented for the complete characterization of the thermoluminescence response obtained from semi-infinite slabs of thermoluminescent phosphors upon exposure to localized Gaussian laser heating beams.

A number of different phosphor configurations are described as examples. These include LiF:Mg,Ti (TLD-100, Harshaw Chemical Corporation) in form of chips, which are widely used in the dosimetry of ionizing radiation, and

DD FORM 1 JAN 73 1473 EDITION OF 1 NOV 68 IS OBSOLETE
S/N 0102-LF-014-6601

SECURITY CLASSIFICATION OF THIS PAGE (When Data Entered)

thin-layer dosimeters prepared either as self-supporting films of powder in a polyimide matrix, or on substrates of LiF single crystals or borosilicate glass. It is demonstrated that all relevant optical and thermal properties of the dosimeters can be determined by these methods and that, based on this knowledge, the expected thermoluminescence response of a given configuration can be simulated as a function of a number of experimental parameters.

For the investigation of the dependence of the thermoluminescence emission yield for a given dose on the heating rate and for experimental tests of the developed theory of heating continuous dosimeter configurations with a beam of uniform intensity profile, a new thermoluminescence laser heating facility was designed and constructed. It features an advanced closed-loop laser control electroncis, a 40 Watt laser, and a uniform round beam of 3 mm diameter or a square one (selectable) of 3 x 3 mm^2 area. This apparatus is described in Appendix C.

INVESTIGATION OF BASIC CHARACTERISTIC OF LASER HEATING IN THERMOLUMINESCENCE AND OF LASER-STIMULATED LUMINESCENCE

Contract No. N0001 4-82-K-0529

Principal Investigator
P. F. Braunlich

Washington State University
Department of Physics
Pullman, WA 99164-2814

ANNUAL REPORT

7/15/84 - 7/14/85

P. F. BRAUNLICH
A. ABTAHI
P. KELLY
J. GASIOT

MARCH 15, 1985

WSU PROJECT NO. 0112

RESEARCH GOALS

The purpose of this research effort is the investigation of the basic characteristics of two differnt types of laser-stimulated luminescence phenomena in view of potential applications in the dosimetry of ionizing radiation and of radiation imaging.

The first of these, laser-heated thermoluminescence, was the subject of the research described in the present Annual Report. The second phenomenon will be the main subject of our studies in the next contract period.

The heat transfer mechnanism from a CO_2 laser beam, having a Gaussian intensity profile, to a semi-infinite thin thermoluminescence phosphor layer and the resulting luminescence response has been studied in detail. Experimental and computational methods were developed for the chacterisation of a given thermoluminescence dosimeter configuration. All its relevant optical and thermal properties can be determined by these methods. Based on this knowledge, the expected thermoluminescence response can be computer-simulated as a function of a number of experimental parameters. This in turn provides a tool to optimize the dosimeter design for applications in dosimetry.

I. Introduction

In recent years the feasibility of heating thermoluminescent materials with infra-red laser beams has been demonstrated [1-4]. This new thermal stimulation method has received particular attention in thermoluminescence dosimetry (TLD) of ionizing radiation because it holds promise as a solution to a number of problems associated with the measurement of small doses of nonpenetrating radiation such as low energy beta rays as well as knock-on protons produced by fast neutrons in hydrogenous radiators [5-7]. Even the imaging of spatial dose distributions of Y-rays and x-rays has been contemplated [1,2] and experimentally demonstrated [8].

The successful development of practical laser-heated TLD readers and thermoluminescence imaging devices, requires detailed knowledge of the heat transfer mechanism from the laser beam to the thermoluminescent sample and the resulting spatio-temporal temperature distribution. Then one may compute and predict the thermoluminescence response (glow curve) of the sample dosemeter for a given laser heating beam [9]. The effects of such interrelated design parameters as laser power density, time of laser exposure, laser beam diameter and intensity profile, sample configuration and composition, and the expected incandescent background emission can be computer-simulated and the resulting glow curve compared with experimental results.

The list of experimental parameters is narrowed down to the few that presently appear important for practical applications. For example, the laser power of cost-effective modern RF or DC discharge excited CO_2 waveguide lasers or RF excited unstable resonator lasers is limited to less than 100 Watts. Laser beam profiles are normally Gaussian intensity distributions or the characteristic annular cross section ("halo") that is possible with an unstable resonator cavity. Uniform beam profiles are highly desirable, but all known methods to produce such beams appear to be impractical in TLD applications because

of the associated power loss or the required custom fabrication of expensive special optics [10].

Suitable dosemeter configurations are thin layers of the TLD phosphor, either in the form of a self-supporting film composed of a high temperature polymer mixture with phosphor particles, or applied to a thin substrate. Both may take the form of discrete circular spots whose diameter is smaller than the full-width at 1/e-power of the laser beam or may be prepared as continuous layers whose area is much larger than the laser beam diameter. However, even the widely used square TLD chips (e.g. the configurations supplied by Harshaw/Filtrol [11]) or round pellets [12] can be successfully heated with a CO_2-laser beam [13].

Small discrete dosemeters can be heated quite uniformly with Gaussian beams provided the laser photons are not too strongly absorbed (uniform heating in the direction of laser propagation). Strongly absorbing dosemeter layers (surface heating) must be thin enough that the thermal response time [14] of the sample is much shorter than the total heating time required to release all trapped carriers. A necessary condition for a spatially uniform temperature rise in both cases is, of course, that the diameter of the discrete spot is much smaller than the diameter of the laser beam. Obviously, a considerable fraction of the laser beam energy is wasted in this mode of operation which, for this reason, will probably be considered only in special situations.

Continuous dosemeter layers are of practical interest because of the ease with which they can be fabricated and because of their potential usefulness in a number of the new applications mentioned above. A localized Gaussian beam can be employed to rapidly heat a small spot on the TLD layer, yielding a characteristic glow curve that is the result of the non-uniform spatio-temporal temperature distribution $T(x,y,z,t)$ produced in this way. This type of thermoluminescence response is completely different from the conventional glow curves obtained by uniform contact heating (an example is shown in Fig. 9 below). It is nevertheless very useful in dosimetric and imaging applications of thermoluminescence [15].

In this paper we present the theory of the thermoluminescence response curves generated with Gaussian laser beam profiles in a number of dosemeter configurations that are of practical importance in thermoluminescence dosimetry. The theoretical approach is verified by comparison with experimental results. In addition, experimental methods are presented for the determination of all relevant thermal and optical properties of the dosemeter materials. Thus, the thermoluminescence response of a given type of dosemeter is completely characterized and the effects of such design parameters as layer thickness, laser power and beam size, pre-annealing temperature and duration, substrate material and its thickness can all be assessed by computer simulation. The special case of a semi-infinite LiF slab has been reported previously [9].

II. THERMOLUMINESCENCE KINETICS FOR NONUNIFORM SPATIO-TEMPORAL TEMPERATURE DISTRIBUTIONS

1. GENERAL REMARKS

Calculations of thermoluminescence glow curves on the basis of simple electron kinetic models and for spatially uniform heating pose no principle problems. While only special cases yield analytical solutions for the thermoluminescence intensity as a function of time or temperature, numerical solutions can readily be generated for the coupled nonlinear rate equations which describe a given trap model [16,17]. The extreme heating rates possible with lasers have been shown not to invalidate the electron-statistical foundation (Shockley-Read statistics [18,19]) of these phenomenological theories [4].

Usually a number of different physically plausible electron-kinetic models will give satisfactory fits of experimental

glow curves. This general lack of uniqueness renders trap-level spectroscopy by monitoring thermally simulated electron-kinetic relaxation phenomena a nontrivial task [16,17]. Spatially nonuniform heating significantly increases the required computational effort and further complicates this situation. For this reason, laser heating techniques are explored herein for the sole purpose of assessing their utility in the dosimetry of ionizing radiation. No attempt is made to verify a given simple trap model or to extract new methods which might facilitate trap-level spectroscopy. Thus, all that is required for our purposes is one reasonably plausible model description for the thermoluminescence kinetics of a suitable phosphor heated with a laser.

The calculations presented here are based on simple Randall-Wilkins first-order kinetics [16]. As the example for a typical phosphor, we choose the most widely used dosimetry material LiF:Mg,Ti (TLD-100) [12]. Experimental fits of its prominent glow peaks (costumarily labelled peaks 2 through 5) have been reported by a number of authors, most recently by McKeever [20] and by Vana and Ritzinger [21]. The fact that the numerical fitting parameters, notably the trap depths and the frequency factors, differ significantly in these papers only underlines the problems associated with curve fitting as a method to obtain basic physical information from thermoluminescence experiments alone. We have arbitrarily selected McKeever's data for our investigations.

2. COMPUTATIONAL APPROACH

Having selected a group of glow peaks in TLD-100 and a suitable, albeit, not unique, fit for modelling these peaks under various experimental conditions, the main task is the calculation of the time evolution of the temperature ("heating program") for each volume element dxdydz at location (x,y,z) of the sample.

A rich literature exists in the field of laser heating of materials. For example, laser annealing of semiconductors has become

an important manufacturing tool in the electronics industry [22-27]. Laser absorption calorimetry of very transparent optical materials also requires the knowledge of the time-dependent temperature distributions produced in the sample [28]. Important insight in the laser damage properties of high-power metallic and dielectric mirrors and other optical components has been gained by studying the theory of laser heating [29,30]. Comprehensive treatments of heat conduction in solids and associated boundary value problems are the texts by Carslaw and Jaeger [31] and Ozisik [32]. However, despite an extensive bibliography on laser heating, the problem of heating thermoluminescence dosemeters with a Gaussian beam turned out to be a unique new case. It is perhaps most closely related to the one solved by Bernal [28] who considered Gaussian beam heating of extremely weakly absorbing cylinders and semi-infinite slabs. The laser beam is, in first approximation, unattenuated when traversing the entire thickness of the slab. Unfortunately, this special case is of little interest here. Weakly absorbing thermoluminescence dosemeter layers are not suited for practical applications because of inefficient use of costly beam energy. Strong to moderate beam attenuation in the active layer is characteristic for laser heating in thermoluminescence dosimetry. However, this problem can be solved analytically by the Green's function method under the assumption that the layer is semi-infinite in radial direction (local heating of a small spot on a large area) and that no significant heat loss occurs due to convection and radiation [9]. Convection can easily be eliminated by evacuation of the sample chamber and radiative losses are indeed small considering the fact that the maximum temperatures of interest do not exceed 700K and the heating times are limited to a few hundred milliseconds. For these assumptions to be valid, the rate of energy absorption from the laser beam must be significantly greater than that of radiative energy loss.

The resulting spatio-temporal temperature distribution is cylindrically symmetric around the beam axis. To calculate the total thermoluminescence emission as a function of time after onset of the

laser exposure, the time-dependent contributions from volume elements $2\pi r\Delta r\Delta z$ are summed by numerical integration over the radial coordinate r and the direction of laser beam propagation z. Because these heating rates are nonlinear in time, analytic solutions of the electron kinetic rate equations for each of these infinitesmial volume elements and their individual unique heating rate are unavailable even for simple first-order kinetics. Therefore, the rate equations must be solved numerically on the basis of the individual temperature evolution of each of these volume elements and their contribution to the emission intensity I(t) must be summed up.

The typical situation encountered in heating a small area of a continuous semi-infinite layer of thickness L by a Gaussian laser beam of intensity

$$I(r,z) = I_o \exp(-r^2/w^2-\mu z) \qquad (1)$$

is schematically depicted in Fig. 1. The symbols chosen are the full width, 2w, at 1/e-peak power of the beam, the absorption coefficient, μ, the radial distance, r, from the axis, and the distance, z, from the front surface upon which the beam is incident. If the beam is turned on at t=0, the temperature distribution T(r,z,t) evolves as a consequence of energy absorption and thermal diffusion, resulting in a spatially resolved time-dependent thermoluminescence emission pattern $I_{TL}(r,L,t)$ similar to the special case shown in Fig. 2. These photographs were obtained by heating a highly absorbing 1mm thick glass slab whose back side at z=L was coated with a 50μm thick layer of ZnS:Cu powder. Here the thermoluminescence emission, $I_{TL}(r,z,t)$, is

not due to direct laser heating of the phosphor itself. Instead, the thermoluminescent layer is heated by temperature diffusion through the glass. Similar experiments were described previously [2]. After appropriate calibration such a thermoluminescence layer can be used to measure the time evolution of isotherms during laser heating of materials. For example, the diameter of the dark center spot in Fig. 2b - 2c corresponds to the 438K isotherm because the thermoluminescence emission of ZnS:Cu, measured by conventional uniform slow heating at a constant heating rate of 15.3K/s, ceases at this temperature. Note that the average heating rate in the laser experiment (Fig. 2) is about the same as can be discerned from the appearance of the dark center spot at about 10s. Other isotherms may be selected as well. For example the peak emission (region of maximum brightness in Fig. 2) corresponds to approximately 381K. Still other emission intensities, measured relative to the peak emission, may be chosen. Actually, the entire temperature distribution present at a given time after onset of heating can be determined by comparison of the normalized emission intensities in Fig. 2 with those of the conventional glow curve measured at approximately the same heating rate.

In dosimetry applications of laser heating the emission, integrated over the total sample volume, is measured with a photomultiplier tube without spatial resolution:

$$I_{TL}(t) = \int\int dr\,dz\; I_v(r,z,t) \qquad (2)$$

Here I_v is the thermoluminescence emission intensity per unit volume.

As a first step in the theory of this TL emission we calculate $T(r,z,t)$ by solving the thermal diffusion equation [9].

$$\nabla^2 T(r,z,t) + k^{-1} g(r,z,t) = \alpha^{-1}\, dT/dt \qquad (3)$$

for the following boundary conditions:

a) The slab is infinite in radial direction and has a thickness L.

b) No heat loss occurs at the boundaries z=0 and z=L, i.e. $\partial T/\partial z = 0$.

This assumption is valid in vacuum in the absence of radiative heat loss.

The initial condition is $T(r,z,t)=T_o$, i.e. room temperature when the laser beam is turned on at t=0. Then the temperature obtained from Eq. (3) is the actual temperature increase above T_o. The notation used in Eq. (3) is as follows:

k = thermal conductivity,

$\alpha = k/\rho c$ = thermal diffusivity,

ρ = mass density,

c = specific heat,

$g(r,z,t)$ = laser power per unit volume present at position (r,z) during laser exposure (source function).

The case of temperature dependent k and α is discussed in Appendix A.

Correcting for reflective loss on the front surface at z=0, the source function g becomes

$$g(r,z,t) = \mu (1-R) I_o \exp(-r^2/w^2 - \mu z) \quad \text{for } t \geq 0$$
$$= 0 \quad \text{for } t < 0, \tag{4}$$

where R is the reflectivity.

We solve Eq. (3) with the initial and boundary conditions stated above by the Green's function technique [32]. The general solution is

$$\Delta T = T(r,z,t) - T_o = \frac{\alpha}{k} \int_{\tau=0}^{t} d\tau \int_{r'=0}^{\infty} r'dr' \int_{z'=0}^{L} dz' \; x$$
$$\left[G(r,z,t;r',z',\tau)\, g(r',z',\tau)\right] \tag{5}$$

where G is the following Green's function:

$$G(r,z,t;r',z',\tau) = \int_{\beta=0}^{\infty} d\beta e^{-\alpha\beta^2(t-\tau)} \beta J_o(\beta r) J_o(\beta r') \; x$$

$$\left[\frac{1}{L} + \frac{2}{L}\sum_{m=1}^{\infty} e^{-\alpha\eta_m^2(t-\tau)} \cos(\eta_m z)\, \cos(\eta_m z')\right] \qquad (6)$$

Here J_o is the zero-order Bessel function and $\eta_m = m\pi L^{-1}$. After integration over r', z', and β, one obtains with $P = \int_o^{\infty} I(r,0) 2\pi r dr = \pi w^2 I_o$ (total power incident on the front surface of the thermoluminescent layer at z=0) the temperature distribution [9]:

$$\Delta T = \frac{(1-R)\alpha P}{kL\pi} \int_{\tau=o}^{t} d\tau \; \frac{e^{-r^2/[4\alpha(t-\tau) + w^2]}}{4\alpha(t-\tau) + w^2} \; x$$

$$\left\{1 - e^{-\mu L} + 2\sum_{m=1}^{\infty} \frac{e^{-\alpha\eta_m^2(t-\tau)}}{1+(\eta_m/\mu)^2} (1 - e^{-\mu L}\cos m\pi)\, \cos(\eta_m z)\right\} \qquad (7a)$$

Note again that Eq. (7a) is the temperature in excess of the initial temperature T_o. The properties of $\Delta T(r,z,t)$ in Eq. (7a) can be readily appreciated by discussing two limiting cases for the absorption coefficient μ. Weak absorption, that is $\mu L \ll 1$, means uniform energy absorption in z-direction. The z-dependent term in the second bracket vanishes and the remaining factor $(1 - e^{-\mu L})$ is simply the fraction of the energy absorbed from the transmitted Gaussian beam. Diffusion broadens the beam profile with increasing time. Very strong absorption, that is $\mu L \gg 1$, means only a thin layer on the surface at z=0 is directly heated and bulk heating occurs only by thermal diffusion. This case is of interest for certain practical dosemeter configurations.

The actual computer simulations make use of the heating rate of each volume element $2\pi r\Delta r\Delta z$, calculated from Eq. 7a:

$$dT/dt = \frac{(1-R)\ \alpha\ P}{kL\pi} \frac{e^{-r^2/[4\alpha t + w^2]}}{4\alpha t + w^2} x$$

$$\{1-e^{-\mu L} + 2 \sum_{m=1}^{\infty} \frac{e^{-\alpha \eta_m^2 t}}{1 + (\eta_m/\mu)^2} (1-e^{-\mu L}\cos m\pi) \cos(\eta_m z)\} \qquad (7b)$$

The four first-order differential equations which describe the independent processes of peaks 2 to 5 [20] were solved together with the heating rate of Eq. 7b by the Runge-Kutta method for each cell $\Delta r \cdot \Delta z$. Sufficient precision was obtained with $\Delta r = 2w/50$, $\Delta z = L/50$ and $\Delta t = 10^{-3}$ x the total exposure time. The sum of the relative peak heights [20] was used a measure of the total trapped electron population and each peak height was normalized by this sum to provide the initial conditions for the TL differential equations. Annealing of the lowest temperature peak # 2 or any other is easily simulated by putting its relative height to zero.

3. EXPERIMENTAL PROCEDURE

The facility shown schematically in Figure 3 was constructed for the measurement of laser stimulated thermoluminescence response curves.

A radio-frequency excited CO_2 laser (Laakmann Electro-Optics, rated at 4 Watts) delivers a cw beam of 1.3mm full width at 1/e-maximum. Together with all the required optical elements and positioners, this laser is mounted on a sturdy aluminum table.

The electromechanical shutter is the first optical element in the laser beam path. To avoid thermal distortion of the shutter blades, they are gold plated for high reflectivity. During the closed position of the shutter, the laser beam is reflected from the blades into a beam dump which simply absorbs and dissipates the laser power. The shutter has a DC power supply which is housed inside the electronic control enclosure. The electronic controlled shutter is open only to heat a sample on the sample holder or to measure by a powermeter the laser power delivered to the sample. The powermeter is mounted on a shaft which slides through the light tight box.

Following the laser beam path beyond the shutter, a 5x beam expander is mounted on the reader table. It can be adjusted to produce various beam diameters (1.5 to 6mm full width) entering the focusing cube. The focusing cube deflects the beam by 90 degrees through an AR coated germanium window and causes it to converge on the TL sample in the light tight box. The germanium window is transparent at the 10.6μm laser wavelength, but opaque to visible light. The beam position on the TL sample is determined by moving the sample holder with two connected x-y translation stages. The translation stages have two actuators which are driven by the Newport Corporation model 350M motor drive system and give an accuracy of the beam position up to 0.1μm.

The TL sample is heated as it absorbs this infra-red radiation from the laser. The high power density of the focused laser beam causes the selected spot on the TL sample to be heated rapidly, while the reminder of the sample remains cool.

The TL emitted by the sample passes the sample substrate and reaches into the photomultiplier tube (PMT) below. The PMT is protected from two types of accidental exposure, one due to the laser by a glass window which will absorb the 10.6μm laser beam, another one due to the visible light (when the sample chamber is open) by a thick aluminum slide. The PMT is an EMI type 9924B with a 1" diameter bialkali photocathode. The current signal from the PMT is digitized, stored and displayed by a Data Precision 6000 Universal Waveform Analyzer (transient digitizer).

The laser TLD reader was designed to permit examination of a number of experimental parameters related to laser heating TLD, e.g., the laser power density that the sample receives, and the beam diameter which is set by mechanically adjusting the beam expander. Laser power and heating time are controlled by settings in the electronic control unit (Fig. 4).

The timing circuits in the electronic control unit consist of four LM555 timers that generate four timing pulses. The first pulse drives

the cycle indicator and limits read cycles to one per second. The second pulse is used to turn the laser off and open the shutter. The third pulse turns the laser on for a precise preselected timing interval. The transient digitizer is triggered at the beginning of this pulse, and the laser is turned off at its end. The fourth pulse triggers the closing mechanism of the shutter. The laser power during the third timing pulse is determined by modulation control. Whenever all four of these pulses are off, the laser operates in a cw mode at maximum output power to maintain a stable operating temperature.

The modulation circuit consists of a 10 MHz Oscillator that triggers a variable length pulse generator. The modulation control is used to vary the pulse width of the resulting pulse train, permitting the laser output power to be varied over a range from zero to full power. The modulation driver amplifies the modulation signal to the 6 volts pulse height required for the laser RF power supply. The shutter control signal and the data signal are both logic level signals. The 74LS series TTL logic circuits are employed for all control logic.

As will be demonstrated below (see for example Fig. 12), the shape of the thermoluminescence response curve depends critically on the laser beam profile in the sample plane at z=0. For this reason we have given its precise measurement particular attention, using the so-called scanning knife edge method [33].

A photodetector measures the laser power not occluded by a knife edge, scanning through the beam, as a function of position. The spatial profile is then given by the first derivative of the photodetector signal with respect to the scan direction. A necessary requirement is that the mathematical form of the profile be separable in the coordinates perpendicular to, and parallel to the scan directions as in the case of a Gaussian.

To check for deviations from circular symmetry, we have always scanned in two perpendicular directions. For cw lasers this procedure is readily executed by scanning at a constant rate and analog

differentiation with an appropriate RC circuit [34]. However, for infra-red lasers such as the one used in our work, thermal detectors are commonly employed to monitor the beam power. Because of their saturation characteristics they are generally not suitable for scanning knife-edge applications. Modifications of this method are required. They are shown schematically in Fig. 5. The cw beam is chopped with the electro-mechanical shutter [3] driven by an oscillator. The oscillator output is used simultaneously as a clock for a transient digitizer (Data Precision model DP 6000) to synchronize the sampling interval with the occurance of the signal pulse from a piezoelectric detector (Barnes Engineering model 350 PZT). In our case the shutter is opened every 73.5ms for 3.5ms. The recorded detector signal during a complete scan has the appearance of a digitally recorded cw signal, exhibiting only the slow temporal structure due to increasing occlusion of the beam by the knife edge. This signal is then differentiated mathematically by the microprocessor of the DP 6000.

Examples of beam profiles obtained in this fashion are shown Fig. 6. The combination of the beam expander and 5" focal length focusing cube afforded variations of the laser spot size in the sample plane between 0.3mm and 2.22mm. The long focal length of the cube and the maximum laser beam penetration depth in our samples of less than 300μm implies that the laser beam profile is independent of the z-direction.

In the following Sections we present experimental results obtained with a number of different dosemeter configurations and comparisons with theoretical calculations.

Case 1: LiF:Ti;Mg Chip

Laser heating of microcrystalline hot-pressed TLD-100 dosemeter material produced by the Harshaw/Filtrol Corporation [11] is of interest as it is widely employed in routine personnel dosimetry. From a theoretical point of view this case is important because of the

rather modest absorption coefficient (μ=40 cm^{-1}) of LiF for 10.6μm photons. The laser beam penetrates 250μm (1/e attenuation depth) into the 900μm thick chip. As it turns out, none of the previously reported solutions of the heat flow equation (Eq. 3) covers this situation in conjunction with a Gaussian heating beam.

Unfortunately only small chips (3mm x 3mm x 0.9mm) are commercially available and, therefore, care has to be taken not to violate the assmuption of a semi-infinite medium (see Section II) when comparing computed with experimental results. In practice this can be done by choosing a beam diameter that is much smaller than the width of the sample and by limiting the total exposure of the laser heating beam to a time during which the sample edges have not yet been heated by thermal diffusion. In order to reach, during this time, in the center of the exposed area the highest temperature peak (peak # 5), the power density in the beam center must exceed a minimum value. In essence this requirement means that a substantial part of the chip volume must be heated to above the maximum temperature for which TL emission will still occur before the edge areas experience any temperature increase by thermal diffusion. We have performed these experiments successfully with beam diameters around 0.084cm and approximately 5 Watt power. Under these conditons a 300ms exposure time raised the temperature at the edges by only a few degrees K above room temperature. Continued exposure to the heating beam beyond this time resulted in heat pile-up in the chip and eventual increase of the temperature of the total sample to above 700K, a situation not covered by the theory presented in Section II.2. However, these experiments are perhaps important as they indicate that entire TLD-100 or similar chips can indeed be heated with an appropriate laser beam so as to measure the total thermoluminescence emission. In fact we have been able to heat these chips to 600K within about 2 seconds with a 2.5mm diameter beam of approximately 8 Watt power.

The temperature distribution established at the end of the exposure (300ms) of a LiF chip to a 0.084cm full width at 1/e-maximum

of 4.93 Watts power is depicted in Fig. 7. Isotherms, calculated from Eq. 7a are shown for temperatures corresponding to the peak temperatures of peaks 2 through 5 (383K, 421K, 457K, and 483K, respectively). The volume inside the 483K-isotherm is heated to temperatures for which thermoluminescence emission from peaks 2 through 4 has ceased at 300ms. Fig. 7 illustrates the nonuniformity of both the temperature distribution and, albeit indirectly, the thermoluminescence emission pattern.

We have made no attempts in our experiments to measure the spatial distribution of the time-dependent thermoluminescence response of the TLD-100 chip to the Gaussian heating beam. Instead the total emission $I_{TL}(t)$ was monitored with a photomultiplier tube and compared with computations performed with the theory outlined in Section II.2. The results are presented in Fig. 8 for a TLD-100 chip that was pre-annealed to 373K for ten minutes in order to remove peak 2. This type of thermal treatment after exposure to the ionizing radiation and before measuring the thermoluminescence glow curve is customary in dosimetry applications of this material. The agreement between the calculated and experimental glow curve is rather satisfying in light of the uncertainties concerning the exact electron-kinetic model description of the thermoluminescence emission from this material and the fact that the TLD-100 chip is not a single crystal as assumed in the calculations. An additional uncertainty stems from the rather strong temperature dependence of the thermal conductivity, k. According to Men et al. [35] k decreases with increasing temperature approximately as T^{-1}. The calculated curve shown in Fig. 8 was obtained with k=0.0275 W/cmK, which is approximately one third of the value measured for a single crystal at room temperature. We have also performed the calculation with an exact solution of the heat flow equation with $k(T)=k_o T_o/T$ using Kirchhoff transformation techniques (see Appendix A). However, no significant improvement in the agreement between measured and calculated thermoluminescence response curves was obtained, perhaps indicating that unaccounted for experimental factors

influenced the results more than an improved theory of heat conduction. We suspect that the micocrystalline "ceramic" nature of the sample and the roughness of the unpolished surface caused some deviations from the implicit assumption that the optical and thermal properties of this material are very close to those of single crystalline LiF. Scattering of the laser light probably results in some broadening of the Gaussian beam profile inside the chip, and the thermal conductivity may be lower than that of a single crystal. In addition, it is well known that, in order to reproduce the exact relative peak heights of peaks 2 to 5 of the TLD-100 phosphor as used in ref. [20], the annealing procedure must be reproduced exactly [12]. Slight deviations might have been present as compared to those used by McKeever [20], resulting in small peak height differences particularly of the low temperature peaks which significantly influence the thermoluminescence response curve obtained by Gaussian beam heating (see Case 4 of this Section).

Case 2: Polyimide foil Loaded with LiF:Mg,Ti Powder

Thin dosemeters are desirable for applications in the dosimetry of low energy beta rays. We have experimented with 84μm thick foils of polyimide (Kapton, DuPont) which were produced by thoroughly mixing TLD-100 powder (grain size 20 to 30μm) with liquid polyimide and spreading this slurry uniformly onto glass slides. After curing for several minutes at 373K and subsequently for 1 hour at 573K, the translucent yellow film was removed by immersion in water. Correcting for the weight loss during the polymerization process, the powder-polyimide weight ratio of the dry foil was about 2:1.

Pieces of 2.5 x 2.5cm^2 size were mounted in metal frames and exposed to γ-rays from a ^{60}Co source. The absorbed dose was 26 Gy. Following a 10 minute pre-anneal at 373K, the thermoluminescence

response curves were measured for a fixed laser power of 4.78 Watts and various laser spot sizes ranging from 0.039 to 0.098cm diameters. A family of curves measured under these conditions is depicted in Fig. 9. Several different sites on the same sample were heated for each laser spot size to assess sample uniformity and laser stability.

All experiments were performed to test the validity of the theory presented in Section II.2 rather than to fabricate viable dosemeters. For example, Kapton absorbs quite strongly the TLD-100 thermoluminescence emission centered around 400nm and, therefore, a foil of this type is rather insensitive as a dosemeter. Nevertheless, important information on the energy transfer from a laser beam to a sample of this type and the resulting thermoluminescence response can be gathered and eventually applied to Kapton foils loaded with TL powders other than LiF.

The TLD-100 loaded Kapton foil does not strongly absorb 10.6μm photons. Yet, direct measurement of its absorption coefficient is not trivial because of the photon scattering off the LiF particles dispersed in it. Since the foil is quite thin and LiF has a rather small absorption coefficient for 10.6μm photons, one can safely assume that the heat deposition is independent of z throughout the entire thickness L. However, scattering introduces an element of uncertainty whose influence on the agreement between theory and experiment can only be estimated by the comparison of measured and calculated thermoluminescence response curves. This case of relatively weak absorption is characterized by $\mu L \ll 1$. As a result, Eq. 7a becomes independent of z:

$$\Delta T = B \int_{\tau=0}^{t} d\tau \, \frac{e^{-r^2/[4\alpha(t-\tau) + w^2]}}{4\alpha(t-\tau) + w^2} \qquad (8)$$

with

$$B = \frac{(1-R)(1-e^{-\mu L})}{\pi \rho c L} P \qquad (9)$$

In attempting to calculate the family of curves in Fig. 9a, the problem of determining the thermal and optical properties of the sample that enter Eq. 8 presents itself. For example, it is not immediately possible to obtain the relevant averaged thermal conductivity, k, for such a heterogeneous mixture from the known values of its components. Also, the total absorbed power $P(1-R)(1-e^{-\mu L})$ is difficult to determine without a suitable calorimeter, while the averaged specific density, ρ, and heat capacity, c, can be calculated in principle from the values of the components.

However the quantity B defined by the entire parameter combination in Eq. (9) can be measured by exploiting the normally undesired onset of incandescent emission that is observed when the sample is exposed to the laser beam significantly beyond the occurrence of the glow curve maximum (see Fig. 9b). We have developed a method for this task that is based on Planck's law of blackbody emission. It makes use of the exponential time dependence of this emission when it is measured for a narrow wavelength interval whose center wavelength, $\bar{\lambda}$, has to be selected in the red or better yet in the infra-red so as to not destroy the sample by overheating it. Also, the experiment has to be performed with significantly higher laser power densities as compared to the ones used in the thermoluminescence experiments in order to assure that the condition $4\alpha t \ll w^2$ is fulfilled so that measurable incandescent emission is generated before the onset of thermal diffusion. Under this condition the temperature rise of the heated spot is linear in time as can be seen from Eq. 8.

$$\Delta T = T - T_o = Bt/w^2 \ , \qquad (10)$$

and it can be shown (see Appendix B) that the so measured incandescent emission intensity, I, obeys the relation

$$(\frac{\partial I}{\partial t})/I = [a/(Bt/w^2 + T_o)^2](B/w^2) \qquad (11)$$

where $a = hc/\bar{\lambda}k$ and T_o is the initial temperature. The quantity B can be calculated by carefully measuring the laser spot size, 2w, and dI/I as a function of time. Details of this method are presented in Appendix B.

For the above mentioned TLD-100-loaded Kapton foils B/P was found to be 5.53 $[Kcm^2/J]$. With this knowledge and the known laser power the thermoluminescence response curves of Fig. 9a can be calculated from Eq. 8 and the computational procedure for glow curves obtained with locally non-uniform heating as described in Section II. This was done by normalizing a single member of a set of curves measured for different laser beam diameters, 2w, and selecting a value for the unknown thermal diffusivity, α, so as to obtain the best fit for all members of the set. Usually a rather good fit is possible for the curves measured with large power densities of the laser beam (e.g. in the present case smaller spot sizes for the fixed laser power of 4.70 Watts). Larger spot sizes tend to yield computed curves that rise later than the experimental ones and are steeper prior to reaching the maximum. Perhaps the scattering of the laser light from the LiF grains, disregarded in our computations, and the associated distortion of the laser beam profile may be a reason for this discrepancy. The value obtained for the thermal diffusivity α=0.0175 cm^2/s appears reasonable in light of the values for LiF (0.02743cm^2/s) and Kapton (0.001cm^2/s).

In closing this discussion of the powder-loaded Kapton foils it may be of interest to mention that the measurement of laser-heated TL glow curves and the developed computational procedure presented in this work

point to a new method for the determination of the thermal properties of otherwise difficult to measure thin-foil TLD dosemeters.

Having completely determined the thermal and optical properties of a given dosemeter of this type, it is relatively straightforward to simulate its thermoluminescence response as a function of other experimental parameters such as laser power, beam diameter, foil thickness, pre-annealing temperature and duration and the like. As an example Fig. 10 shows the dependence on the laser power of the sample from Fig. 9a for a fixed beam diameter $2w = 0.062$cm. Thus, the techniques are now available for the optimization of dosemeter designs for the use in laser-heated thermoluminescence dosimetry readers [3].

Case 3: Thin LiF:Mg,Ti Phosphor Layer on a Glass Slab - a) Heating Beam on Layer

Another dosemeter configuration of potential importance for laser-heated thermoluminescence dosimetry is a thin TL phosphor layer on a substrate that is transparent for the emitted thermoluminescence photons. In this arrangement the heating beam may be directed so as to expose a small spot of the sample on the side that is covered with the active layer and the thermoluminescence emission is monitored with a photon detector on the opposite side. The substrate may be chosen according to its absorption coefficient for the photons of the heating beam. For example BaF, LiF, and sapphire or glass are materials having absorption coefficients increasing in that order. Assuming the phosphor layer is sufficiently thin and composed mainly of TLD-100 phosphor powder, little energy is transferred from the 10.6μm beam using a BaF substrate. However, useful thermoluminescence response curves are obtained with a single crystalline LiF substrate (see Fig. 11). The most efficient utilization of the laser beam energy is achieved by a highly absorbent substrate such as common boroslicate glass. The thermoluminescence response of such a dosemeter configuration is the rather complex result of both direct and indirect

(via absorption by the glass and subsequent diffusion) heating of the phosphor. Both, its optical properties at 10.6μm as well as its thermal characterstics, are due to the contributions of the individual properties of both components in an unknown fashion and are for this reason difficult to measure. However, by applying a layer that is considerably thinner than the substrate and considering the fact that this layer does only moderately absorb the laser photons, heating is mostly indirect via diffusion from the strongly absorbing glass surface. Therefore, one can assume that the thermal diffusivity, α, of the dosemeter is very close to that of the glass (α = 0.0075 cm^2/s). In fact, it should be slightly higher than that of lime glass because of the contribution to the "configuration-averaged" α from the LiF content of the phosphor layer. We have performed all calculations (see below) of the thermoluminescence reponses of thin-layer dosemeter configurations which use borosilicate glass substrates with the value of α = 0.01 cm^2/s (glass composition: 64% silicon dioxide, 13% alkali oxides, 8% boron oxide, and 15% other oxides). The only parameter combination not known for this type of dosemeters is B (see Eq. 9), which is obtained by the best fit of calculated and measured TL response curves.

We have performed experiments with thin uniform TLD-'00 powder layers in a silicone binder on 0.159mm thick borosilicate glass microscope cover slides. An example of such a family of glow curves measured with a fixed laser power and for various laser spot sizes is presented in Fig. 12. A 25 x 25mm^2 slide was coated with a 51μm thick layer of LiF (TLD-100) powder (grain size between 30 and 40μm) in a silicone binder (cured weight ratio 2:1) and exposed to 50 keV x-rays. After 10 min. pre-anneal at 373K to remove peak 2 [20], well separated areas on this sample were exposed to laser heating pulses of 4.45 Watt power and spot sizes of full widths ranging from 1 to 2mm. In order to avoid the onset of incandescent emission from the center of the exposed spot the exposure times were adjusted according to the power density, ranging from 100ms to 250ms. From the best fit of the computed curves to these measurements B was found to be 20 Kcm^2/s for the laser power stated above.

With this value of B other series of thermoluminescence response curves for this type of dosemeter can readily be generated. For example the influence of the laser power P for various spot sizes or the thickness L of the sample can be studied by computer simulation in order to arrive at an optimal dosemeter design for a given available CO_2 laser. An example is presented in Fig. 12b which demonstrates rather large changes in the peak location of the thermoluminescence response curves when varying the laser power by only 10%, indicating the necessity to use a highly stabilised laser beam for applications of laser heating in thermoluminescene dosimetry.

Case 4: Thin LiF:Mg,Ti Phosphor Layer on a Glass Slab - b) Heating Beam on Glass Side Opposite the Layer

It is of course also possible to heat the active thermolumiscent layer through the substrate. Choosing again a relatively thin microscope cover slide interesting thermoluminescence response curves from a TLD-100 phosphor layer were obtained. Compared to those measured by frontal heating with the same laser power and beam diameter, they all peak at a later time because diffusion through the strongly absorbing substrate in now the only mechanism of heat transfer. At the same time the effected spot size is considerably larger.

A series of curves measured with a laser power of ~~4.2~~ 4.18 Watts and spot sizes ranging from ~~1.38~~ 1.65mm to ~~2.22~~ 2.13mm full width is shown in Fig. 13 for the same sample used in the experiments of Fig. 12. The theoretical curves were again computed from Eq. 7b with an experimentally determined value for the parameter combination B=16.75 cm^2/s. The best fit was obtained with a thermal diffusivity of $\alpha=(7.8 \pm 0.5) \times 10^{-2} cm^2/s$. The calculated dependence of the thermoluminescence response on the laser power for a spot size of ~~1.6~~ 1.65mm is plotted in Fig. 14 together with curves calculated for a fixed power and spot size and different sample thickness L.

We have used the same sample in an attempt to study the effect of pre-annealing on the thermoluminescence response curve. These experiments are not just a trivial repetition of what has been done before by many authors to find the appropriate treatment for removal of rapidly fading low temperature glow peaks prior to the dose measurement. Because the temperature distribution is nonuniform when a semi-infinite slab is heated by a localized beam of Gaussian profile, uniform pre-annealing effects the response curve much more severely than the conventional glow curve. This becomes obvious by careful examination of the photographs of Fig. 2 which may be considered as a "coded" temperature distribution in the emitting layer for the various times after onset of the laser exposure. Imagine ring-like surface areas between two adjacent isotherms of a given small temperature difference. At the perimeter of the emission pattern, which is at a low temperature, the emission from such a ring is due to the low temperature peaks of the conventional glow curve. A ring of the same temperature difference, but located closer to the center, emits at the same time at a higher temperature. Assuming for the sake of simplicity identical brightness of these two areas, their contribution to the total emission (monitored with a detector and without spatial resolution) is proportional to the square of their respective radii. Removing the low temperature glowpeaks by uniform pre-anneal treatment affects the outer and, thus, larger emitting area and consequently the strongest contributions to the emission at that time. Fig. 15 is an illustration of this phenomenon. Three thermoluminescence response curves are shown measured with a laser power of 3.63 Watts and a spot size of 1.6mm 1/e-power diameter. The sample is the same as that used to produce the curves of Fig. 13. A 373K pre-anneal of only 5 min., which is known to remove the low intensity peak 2 of the conventional glow curve [20] has a rather large effect on the thermoluminescence response curve measured with Gaussian laser beam heating.

Pre-annealing at the same temperature for 10 min. has almost no measurable effect on peaks, 3, 4 and 5 of the conventional glow curve while the difference can still be detected in curve c of Fig. 15. We refrain here from reporting pre-annealing measurements and computer simulations performed with all the sample types used in our investigations. Instead we restrict ourselves to pointing out that in practical dosimetry applications of laser heating continuous dosemeter layers with Gaussian beam profiles [15] great care has to be taken to reproducibly pre-anneal the samples. In addition, fading of the information on absorbed doses stored in the thermoluminescence dosemeter will cause a similarly enhanced error as compared to conventional contact heating.

III. Conclusions

We have presented the theory of thermoluminescence response curves generated with Gaussian laser beam profiles for a number of practical and interesting dosemeter configurations, and we have verified our theoretical approach by direct comparison with experiment. We have also shown that by computer simulation one can assess the effects of such design parameters as layer thickness, laser power and beam size, pre-annealing temperature and duration, substrate material and its thickness.

The extremely fast heating rates (> 10^4K/s) which can be obtained by laser heating versus that of conventional contact heating in solid-state dosimetry (~ 1K/s) and the reduced amount of phosphor required in our thin film configuration indicate quite clearly that the techniques which we have developed and presented here-in while of interest in their own right will be of significant practical importance.

1. J. Gasiot, P. Bräunlich, and J.P. Fillard; J. Appl. Phys. 53, 5200 (1982).
2. P. Bräunlich, J. Gasiot, J.P. Fillard, and M. Castagne; Appl. Phys. Lett. 39, 769 (1981).
3. P. Bräunlich, S.C. Jones, and W. Tetzlaff; Radiation Protection Dosimetry 6, 103 (1984).
4. P. Kelly, P. Bräunlich, A. Abtahi, S.C. Jones, and M. deMurcia; Radiation Protection Dosimetry 6, 25 (1984).
5. P. Bräunlich, W. Tetzlaff, J. Gasiot, and S.C. Jones; Proceedings of the International Beta Dosimetry Symposium, Washington, D.C. (1983), p. 293 (NUREG/CP-0050).
6. P. Bräunlich, M. Brown, J. Gasiot, J.P. Fillard; Proceeding of the Ninth DOE Workshop on Personnel Neutron Dosimetry, Las Vegas (1982); p. 193 (CONF-820668).
7. V.K. Mathur, M.D. Brown, and P. Bräunlich; Radiation Protection Dosimetry 6, 163 (1984).
8. Y. Yasuno, H. Tsutsui, O. Yamamoto, and T. Yamashita; Japan J. Appl. Phys. 21, 967 (1982).
9. P. Bräunlich, S.C. Jones, A. Abtahi, and M. deMurcia; Radiation Protection Dosimetry 6, 83 (1984).
10. C. Han, Y. Ishi, and Murata; Appl. Optics 22, 3644 (1983).
11. Harshaw Chemical Co., 6801 Cochran Road, Solon, OH 44139.
12. G. Portal; "Preparation and Properties of Principal TL Products", in Applied Thermoluminescence Dosimetry, M. Oberhofer and A. Scharmann, ed., pp. 97-122, Adams Hilger Ltd., Bristol (1980).
13. P. Bräunlich, W. Tetzlaff (unpublished).
14. M. Sparks; J. Appl. Phys. 47, 837 (1976).
15. P. Bräunlich; Final Report "Development of Laser Heating Techniques in Beta Thermoluminescence Dosimetry", Jan. 1984, prepared for the Pacific Northwest Laboratories, Battelle Memorial Institute, Subcontract # B-81227-A-X (unpublished).
16. P. Bräunlich, P. Kelly, and J.P. Fillard; "Thermally Stimulated Luminescence and Conductivity", in Thermally Stimulated Relaxation in Solids, P. Bräunlich, ed., Springer, Heidelberg (1979).
17. P. Kelly, M. Laubitz, and P. Bräunlich; Phys. Rev. 84, 1960 (1971).

18. W. Shockly, W.T. Read, Jr.; Phys. Rev. 87, 835 (1952).
19. P. Bräunlich; "Introduction and Basic Principles" in Thermally Stimulated Relaxation in Solids, Springer (Heidelberg, 1979).
20. S.W.S. McKeever; Nuc. Instr. and Method 175, 19 (1980).
21. N. Vana and G. Ritzinger; Radiation Protection Dosimetry 6, 29 (1984).
22. A.B. Donaldson; J. Franklin Institute 294, 275 (1972).
23. Y.I. Nissim, A. Lietoila, R.B. Gold, and J.F. Gibbons; J. Appl. Phys. 51, 274 (1980).
24. J.R. Meyer, M.R. Kruer, and F.J. Bartoli; J. Appl. Phys. 51, 5513 (1980).
25. J.R. Meyer, F.J. Bartoli, and M.R. Kruer; Phys. Rev. B 21, 1559 (1980).
26. A. Maruani, Y.I. Nissim, F. Bonnouvrier, and D. Paquet; Proceedings of the Symposium on Laser Solid State Interactions and Transient Thermal Proceedings of Materials, Mat. Res. Soc. Symp. Proc. 13, 123 (1983).
27. A. Maruani, Y.I. Nissim, F. Bonnouvrier, and D. Paquet; J. de Physique, Colloque C5, 87 (1983).
28. E. Bernal G.; Appl. Optics 14, 314 (1975).
29. M. Sparks; J. Appl. Phys. 47, 837 (1976).
30. R.E. Warren and M. Sparks; J. Appl. Phys. 50, 7952 (1979).
31. H.S. Carslaw and J.C. Jaeger; "Conduction of Heat in Solids", 2nd ed., Oxford U.P., Oxford, (1959), p. 112.
32. M.N. Ozisik; "Heat Conduction", Wiley, New York (1980).
33. G. Brost, P. Horn, and A. Abtahi; Appl. Optics 24 (accepted for publication).
34. A.H. Firester, M.E. Heller, and P. Sheng; Appl. Optics 16, 197 (1977).
35. A.V. Petrov, N.S. Tsypkina, and V.E. Seleznev; High Temperature-High Pressure 8, 537 (1976).

Figure Captions

Fig. 1 Schematic representation of a Gaussian laser beam profile exposing the surface (z = 0) of a slab of thickness L.

Fig. 2 Thermoluminescence emission pattern obtained from a 50 μm thick uniform ZnS:Cu layer on a 1 mm thick glass slab (25 x 25 mm^2). The sample was heated by a cw CO_2 laser beam of 4.3 Watts and 5.4 mm full width at 1/e peak power. The beam was directed perpendicularly at the center of the glass slab on the side opposite to the phosphor layer. The photographs were taken at the indicated times after onset of the laser exposure.

Fig. 3 Schematic representation of the laser-heated thermoluminescence reader.

Fig. 4 Block diagram of the electronic control system for the apparatus shown in Fig. 3.

Fig. 5 Schematic arrangement for knife-edge scanning of the CO_2 laser beam profile. Note that the position of the knife-edge in the sample plane is shown here vertically because the focusing cube (see Fig. 3) is omitted for simplicity.

Fig. 6 Example of a typical nearly Gaussian spatial profile obtained for the CO_2 laser beam at z = 0 (see Fig. 1).

Fig. 7 Temperature distribution established after heating a small LiF slab of area 3x3mm^2 and thickness L=0.9mm for 300ms. A Gaussian laser beam of 4.93 Watts power and .84mm full width impinges on the center of the slab at z/L=0. The calculations were performed with Eq. 7b and k=0.0275 W/cmK, c=1.56 Ws/gK, ρ=2.635 g/cm^3, and an absorption coefficient for 10μm of $\mu=40cm^{-1}$.

Comparison

Fig. 8 Measured (---) and calculated (solid line) thermoluminescene response curves obtained from the LiF:Mg, Ti (TLD-100) chip of Fig. 7 after x-ray exposure. The calculations were performed with Eq. 7b and the first-order electron kinetic parameters (frequency factor, trap depth) determined by McKeever [20] for peaks 3-5 of this thermoluminescent phosphor. Peak 2 was removed by 10 min. pre-annealing at 373K.

Fig. 9 a) Measured and calculated (solid line) thermoluminescence response curves obtained after x-ray exposure of a 84μm thick polyimide foil loaded with LiF:Mg,Ti (TLD-100) particles of 20-30μm grain size at a polymer-powder weight ratio of 1:2. The curves were measured with a 4.7 Watt CO_2 laser beam of full widths (from left to right) of 0.39mm, 0.62mm, 0.77mm, and 0.985 mm. The calculations were performed with Eq. 8 and B = 26 Kcm^2/s (see Eq. 9) which was determined by the incandescence emission method (Appendix B) at this laser power. The thermal diffusivity of the polyimide-LiF composite was found to be α = 0.0175 cm^2/s by the best fit of the calculation to a series of measured curves obtained with various laser spot sizes but otherwise identical conditions.

Fig. 9b) A set of thermoluminescence response curves obtained with an identical sample as the one used in Fig. 9a except for longer heating times, which were increased to demonstrate the occurrence of incandescence emission. Each curve drops off sharply upon turning off the laser beam.
Laser power: 4.75 Watts
Laser beam diameter 2w [mm] (from left to right): 0.899, 0.942, 0.985, 1.024, 1.063, and 1.102.

Fig. 10 Example of calculated dosemeter performance. The sample is the self-supported polyimide-powder foil from Fig. 10, all optical and thermal properties being identical. The calculations were carried out for a fixed laser spot size at 0.62mm and laser powers P of 10, 5, 4, 3 and 2 Watts. Note that for clarity these thermoluminescence response curves are scaled by dividing the TL intensity by a numerical factor equal to the laser power in Watts.

Fig. 11. Thermoluminescence response curves measured from a uniform LiF:Mg,Ti layer (thickness: 3.7 mg/cm^2, 20μm grain size, Dow Corning 805 silicone binder) on a 0.15cm thick non-thermoluminescent LiF single crystal of 25 x 25mm^2 area.
Laser power: P = 4.95 Watts
Laser spot size 2w(in mm)
1: 0.326, 2: 0.327, 3: 0.330, 4: 0.336, 5: 0.340mm.
To check the reproducibility of the measurements, several thermoluminescence responses from different sites on the sample were measured for otherwise identical conditions. Repeated measurements are shown here only for the largest three of the five different spot sizes chosen for this experiment.

Fig. 12a Thermoluminescence response curves measured with a 4.45 Watts laser beam by heating the phosphor-coated side of a 0.159 mm thick glass slab after x-ray exposure. The 51μm thick coating consisted of TLD-100 powder (grain size 30-40μm) in a Dow Corning 805 silicone binder (2:1 weight ratio). The solid lines are curves computed from Eq. 7b and the first-order electron kinetic parameters determined by McKeever [20] for peaks 3-5. Peak 2 was removed by a 10 min. pre-anneal at 373K.

With the known thermal diffusivity $\alpha=0.01 cm^2/s$ the parameter B was determined by fitting a family of curves obtained for the following full widths, 2w, [mm] (curves from left to right): 2.03, 1.83, 1.65, 1.45, 1.24 respectively.

Fig. 12b Computed thermoluminescence response curves for various laser powers. The sample is identical to that of Fig. 12a. The laser spot size, 2w, is 1.944mm and the laser powers (curves from left to right) are 4.895, 4.45, and 4.005 Watts, respectively.

Fig. 13 Thermoluminescence response cuves of the sample from Fig. 12, however, the laser heating beam impinges onto the side opposite to the phosphor-coated one. Thermal diffusion through the thin glass slab is now required to produce the thermoluminescence emission. With the known thermal diffusivity of this sample (see Fig. 12a) the B parameter (Eq. 9) was determined to be 16.5 Kcm^2/s at P=4.18 Watts by the best fit of computed curves to the entire series of curves measured for different laser beam widths 2w. Again, peak 2 of TLD-100 was removed by annealing. The solid lines are the curves computed with Eq. 7b and on the basis of first-order electron kinetics and the following measured beam widths, 2w [mm]: 1.65, 1.994, 2.13 respectively.

Fig. 14 Thermoluminescence response curves of the sample from Fig. 13 computed from Eq. 7b for various laser powers P and total sample thicknesses L and fixed spot size 2w=1.65mm. Again it was assumed that peak 2 of the TLD-100 phosphor was removed by pre-annealing. The solid curves were calculated for L=0.210mm and the following laser powers (from left to right): 6.27, 4.18, and 3.125 Watts.

The dashed curves demonstrate the effect of the total thickness, L, by increasing the substrate thickness only (fixed phosphor layer thickness of 0.051mm). The calculations were performed with a laser power P=4.18 Watts and the following total thicknesses L (from left to right): 0.105, 0.210, 0.420, and 0.630mm.

Fig. 15 The effect of pre-annealing for 10 min. at 373K on the thermoluminescence response curves obtained from the sample of Fig. 12 by heating it through the glass with P=3.63 Watts and a laser spot size 2w=1.6mm. The first curve (on the left) is obtained without annealing immediately after exposure of the sample to 50 kev x-ray for 4 min. The other two curves represent the TL response after 5 min. and 10 min. pre-annealing at 373K, respectively.

Fig. 16 Determination of $B=(1-R)(1-e^{-\mu L})P/\pi\rho cL$ (see Eq. 9) for powder-loaded Kapton foils by the incandescence method described in Appendix B. Shown are the rise of the incandescence emission, I, (solid line) and its time-derivaive, $(\frac{\partial I}{\partial t})/I$, (dashed line) as a function of time after exposure of the foil (without previous exposure to ionizing radiation to eliminate thermoluminescence emission) to a 4.8 Watt laser beam of spot size 2w=0.118cm $(\frac{\partial I}{\partial t})$. From the ratio $(\frac{\partial I}{\partial t})/I$, determined between zero and .03s, B was found to be 27±3 Kcm^2/s for this laser power.

APPENDIX A

When the thermal conductivity varies with temperature, the non-linear differential equation of heat conduction (compare with Eq. 3) can be written as

$$\nabla.[k(T)\nabla T] + g(r,z,t) = \rho c \partial T/\partial t \qquad (1\text{-A})$$

where the thermal conductivity, k, and the thermal diffusivity, α, are assumed to be temperature dependent; but the heat source function, g(r,z,t), does not depend on temperature.

Equation (1.A) can be linearized by a transformation which involves a change of the dependent variable. This method is called the Kirchhoff transformation [32]. The new variable of transformation, U, is defined as

$$U = \int_{T_o}^{T} \frac{k(T')}{k_o}\, dT'$$

or by

$$\frac{\partial U}{\partial T} = k(T)/k_o, \qquad (2\text{-A})$$

where T is a reference temperature and k_o is the value of k(T) at T_o. Upon substitution, Eq. 1-A becomes

$$\nabla^2 U(r,z,t) + 1/k_o\, g(r,z,t) = 1/\alpha \frac{\partial}{\partial t} U(r,z,t)\ , \qquad (3\text{-A})$$

where $\alpha = k(T)/\rho c$.

For the materials of interest in thermoluminescence dosimetry, the thermal diffusivity, $\alpha = \alpha(T)$, varies very little with temperature and can be assumed constant. The initial and boundary conditions for

Eq. 3-A can be derived from the original conditions [9] using 2-A, and the solution has the same form Eq. 7a.

For the case of LiF [35], the thermal conductivity may be fitted by a function of the form

$$k(T) = T_o/T\ k_o \tag{4-A}$$

In our case, T_o is the room temperature. Then the Kirchhoff transformation gives

$$U = T_o\ \mathrm{Ln}\ (T/T_o) \tag{5-A}$$

and the temperature expression in terms of U can be extracted from Eq. 5-A as

$$T(r,z,t) = T_o\ \exp(U(r,z,t)/T_o) \tag{6-A}$$

where U(r,z,t) is given as:

$$U(r,z,t) = \frac{(1-R)\alpha P}{\pi k L} \int_{\tau=o}^{t} dt\ \frac{e^{-r^2/[4\alpha(t-\tau)\ +\ w^2]}}{4\alpha(t-\tau)\ +\ w^2}\ x \tag{7-A}$$

$$\left\{1-e^{-\mu L}\ +\ 2\ \sum_{m=1}^{\infty}\ \frac{e^{-\alpha m^2\pi^2(t-\tau)/L^2}}{1\ +\ (\frac{m\pi}{\mu L})^2}\ (1-\cos\ m\pi)\ \cos(\frac{m\pi z}{L})\right\}$$

APPENDIX B

The parameter combination defining B in Eq. 9 of Section III.2 contains the thermal properties, the reflectivity, and the absorption coefficient for the TL sample as well as the power of the laser heating beam. In principle, these may be measured separately. However, that turns out to be rather difficult for the self-supporting thermoluminescent foils, because the material is a composite of a powder and a polymer. Therefore, we developed a method to determine B experimentally so as to be able to calculate the temperature distribution T(r,z,t) and the resulting glow curves of these dosemeter configurations, whose total absorption of the laser heating beam is not too large (no dependence on z). It will be shown that it is possible to extract B from the incandescent background emission of the heated spot on the sample.

As described in Section III, incandescent emission from the center hot spot of a sample exposed to the Gaussian laser beam is always present when TL glow curves are measured and the laser beam is not prematurely turned off (see Fig. 9b).

The energy density for a given wavelength λ of the incandescent blackbody emission is given by Planck's law:

$$U_\lambda = 8\pi hc\lambda^{-5}\left[\exp\left(\frac{hc}{\lambda kT}\right)-1\right]^{-1} \qquad (1\text{-}B)$$

where T is the absolute temperature, and h and k have the usual meaning. We tried to keep the temperature below 600K in order not to destroy the sample which visibly darkened by only briefly heating it above that limit. Therefore we can assume $\frac{hc}{\lambda kT} \ll 1$, and Eq. 1-B reduces to

$$U_\lambda = 8\pi hc\lambda^{-5}\exp\left(-\frac{hc}{\lambda kT}\right) \qquad (2\text{-}B)$$

The total intensity I in the spectral range of sensitivity of the photomultiplier tube is given by

$$I_b \alpha \int_{\lambda_1}^{\lambda_2} K(\lambda) U_\lambda d\lambda \qquad (3\text{-B})$$

where $K(\lambda)$ is the quantum efficiency. It turned out to be a linearly decreasing function of the wavelength between 600nm and 650nm, the wavelength interval utilized in our experiments. This yields

$$I_b \alpha \exp(-\frac{hc}{\bar{\lambda} kT}) \qquad (4\text{-B})$$

where $\bar{\lambda}$ is at the center of this sensitivity region which is determined by the photomultiplier and a short wavelength cut-off filter (see below).

In order to eliminate the unknown proportionality constant in Eq. 4-B, one can utilize the ratio of the first derivative with respect to time and this expression. This ratio is readily determined experimentally:

$$(\frac{\partial I}{\partial t})/I \alpha (a/T^2)\exp(-a/T)(dT/dt) \qquad (5\text{-B})$$

and

$$(\frac{\partial I}{\partial t})/I = (a/T^2)(dT/dt) \qquad (6\text{-B})$$

where $a = \frac{hc}{\bar{\lambda} k}$.

The time dependence of the temperature is given by Eq. 8 of Section III.2. We may consider the simplest case which for the temperature is proportional to the time t. This is valid only for $4\alpha t < w^2$ and yields

$$T - T_o \alpha Bt/w^2 \qquad (7\text{-B})$$

Then

$$(\frac{\partial I}{\partial t})/I = [a/(Bt/w^2 + T_o)^2](B/w^2). \qquad (8\text{-}B)$$

The quantity B is calculated by determining this ratio experimentally and careful measurement of the 1/e full width, 2w, of the laser beam.

EXPERIMENT RESULTS

One of the 4 different dosemeter configurations was a polyimide film loaded with LiF powder. Both materials of this 84μm thick composite film absorb the 10.6μm heating photons only moderately. One can, therefore, assume that Eq. 8 is applicable.

The parameter combination B of Eq. 9 is straightforwardly determined by recording the time evolution of the incandescent emission at a narrow wavelength interval around $\bar{\lambda}$. Using a step filter having a low-wavelength transmission cut-off at 600nm (interference filter type 6135-650, Optics Technology, Palo Alto, California). Together with an EMI 9924B PMT yielded $\bar{\lambda}$ = 625nm. The incandescent signal obtained by heating this foil with P = 4.8 Watts and 2 = 0.118cm is shown in Fig. 1-B together with its derivative as obtained by digital processing with the Data Pecision DP6000 waveform analyzer. From the ratio $(\frac{\partial I}{\partial t})/I$, again calculated directly with the DP6000, B was determined to be 27cm² K/s for the laser power stated above. The condition $4\alpha t < w^2$ is fulfilled with the values α = 0.0175cm²/s (see Section III.2), t = .03 sec and w = 0.059 ~~0.6cm~~.

It should be pointed out that the above method is not applicable for the dosemeter configuration described in Sections III.1, 3, and 4 because here the z-dependence of the temperature rise cannot be neglected and Eq. 8 is not valid.

ACKNOWLEDGEMENT

The autnors are indebted to S.C. Jones, W. Tetzlaff, and M. deMucia for their valuable contributions in the early stages of this project, which was sponsored by the Office of Naval Research under Contract No. N00014-82-K-0529.

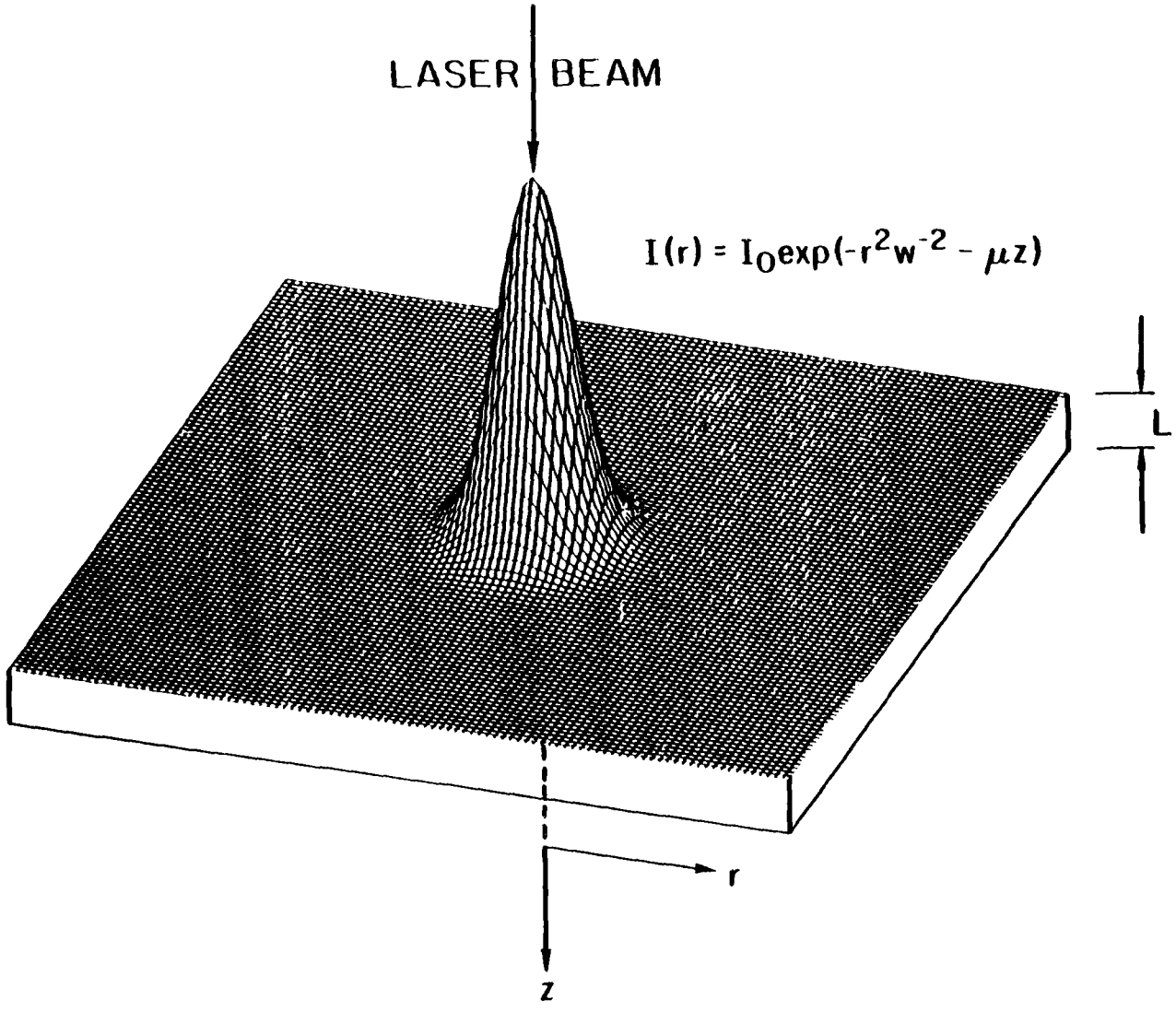
LASER BEAM
$I(r) = I_0 \exp(-r^2 w^{-2} - \mu z)$
L
r
z

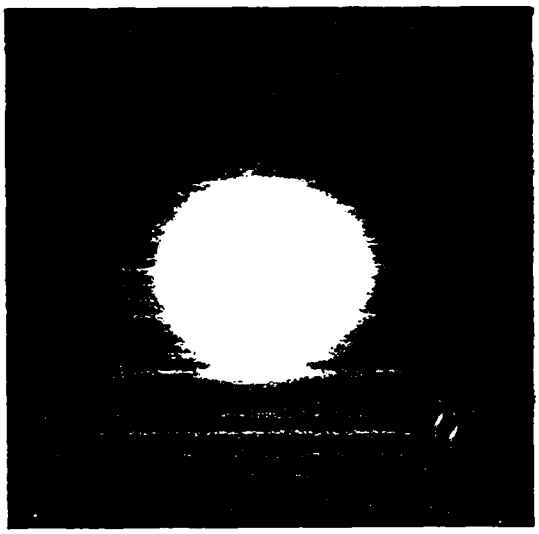

a 5 sec.

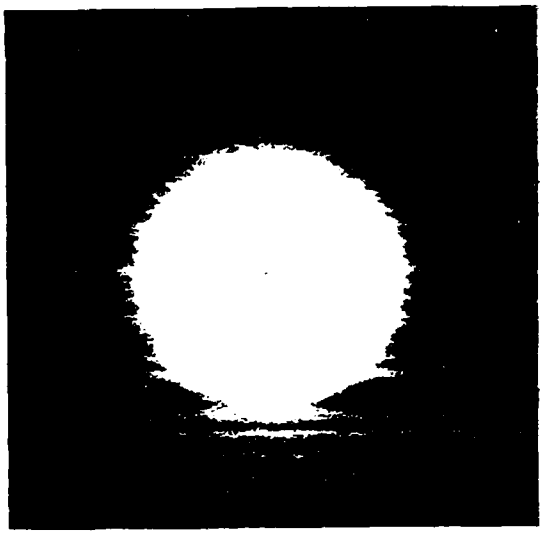

b 10 sec.

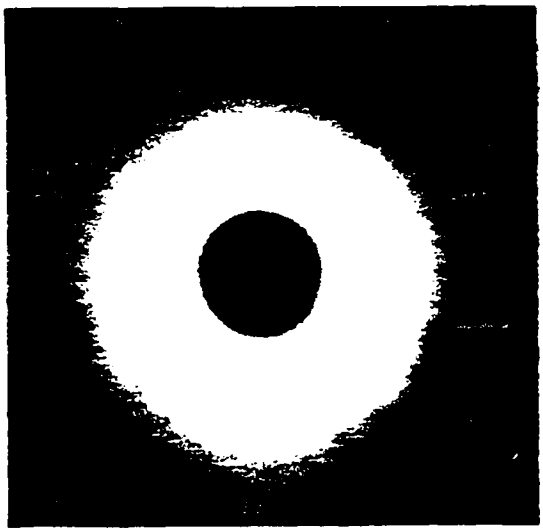

c 22 sec.

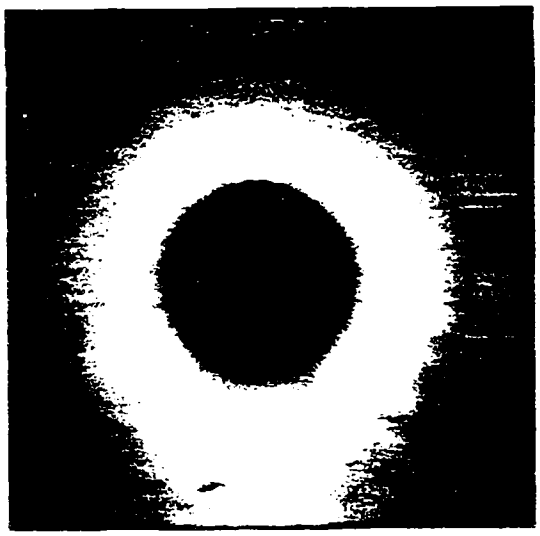

d 35 sec.

25 mm

Fig. 2

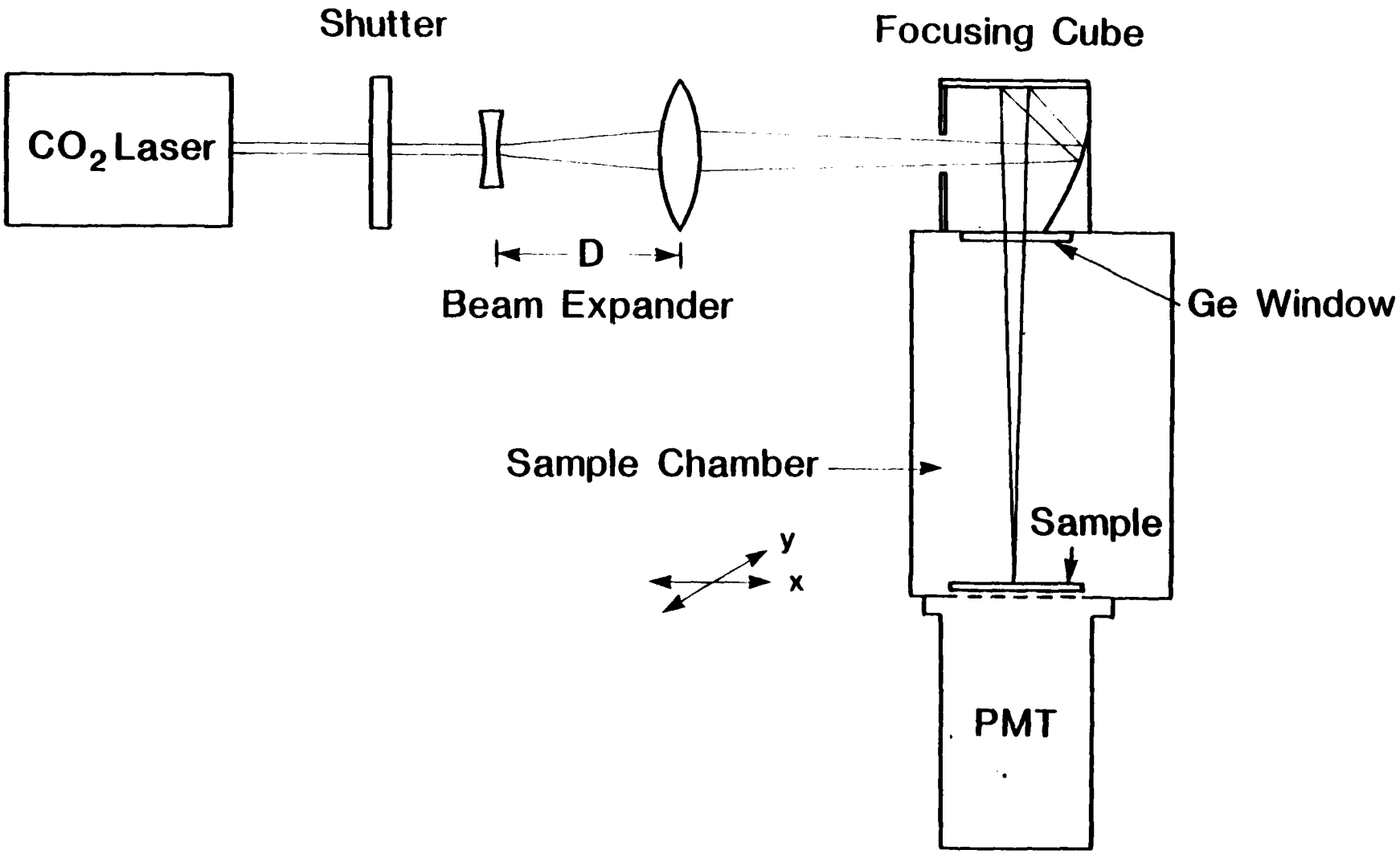
Shutter
Focusing Cube
CO_2 Laser
D
Beam Expander
Ge Window
Sample Chamber
Sample
y
x
PMT

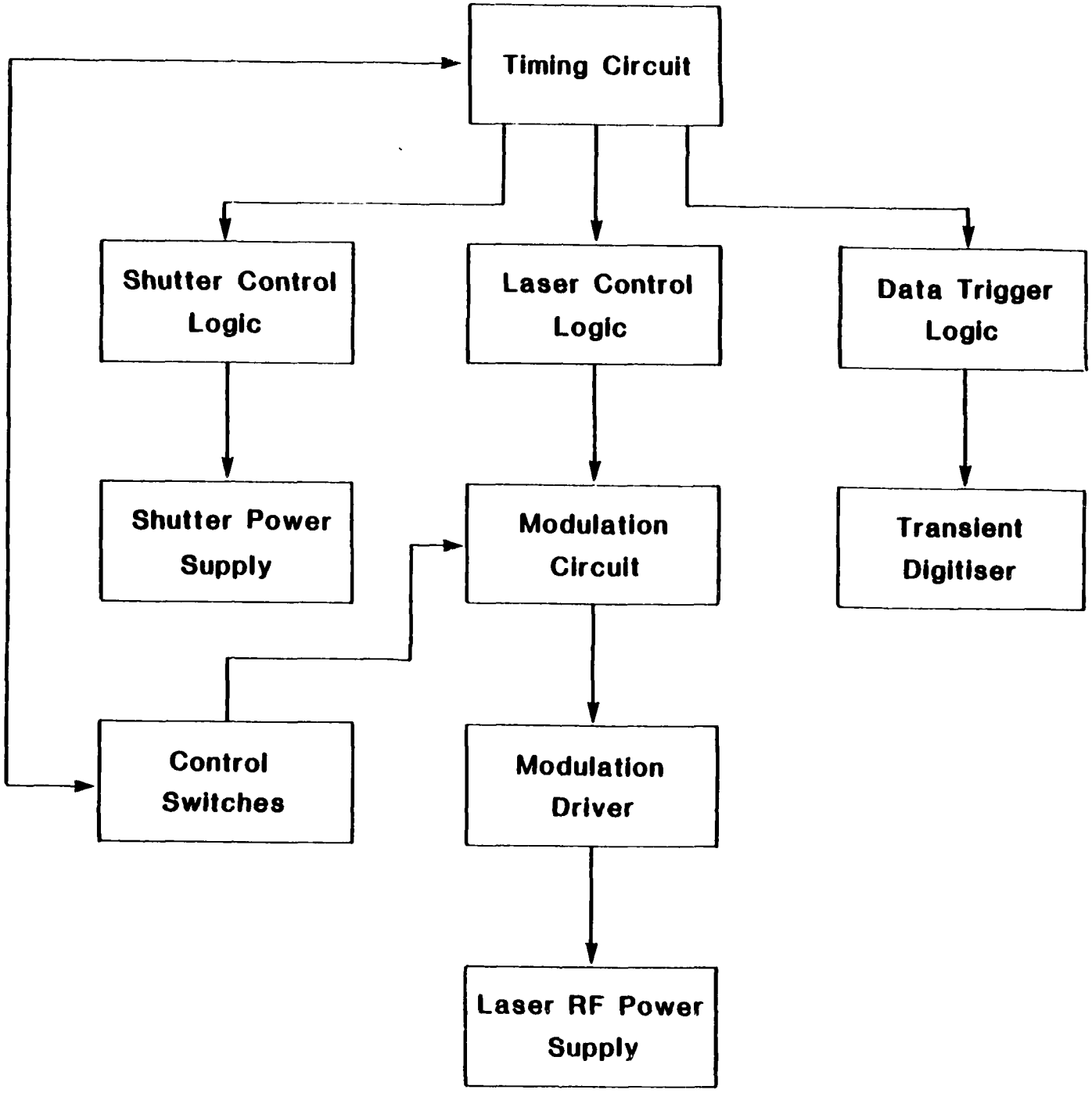
Timing Circuit
Shutter Control Logic
Laser Control Logic
Data Trigger Logic
Shutter Power Supply
Modulation Circuit
Transient Digitiser
Control Switches
Modulation Driver
Laser RF Power Supply

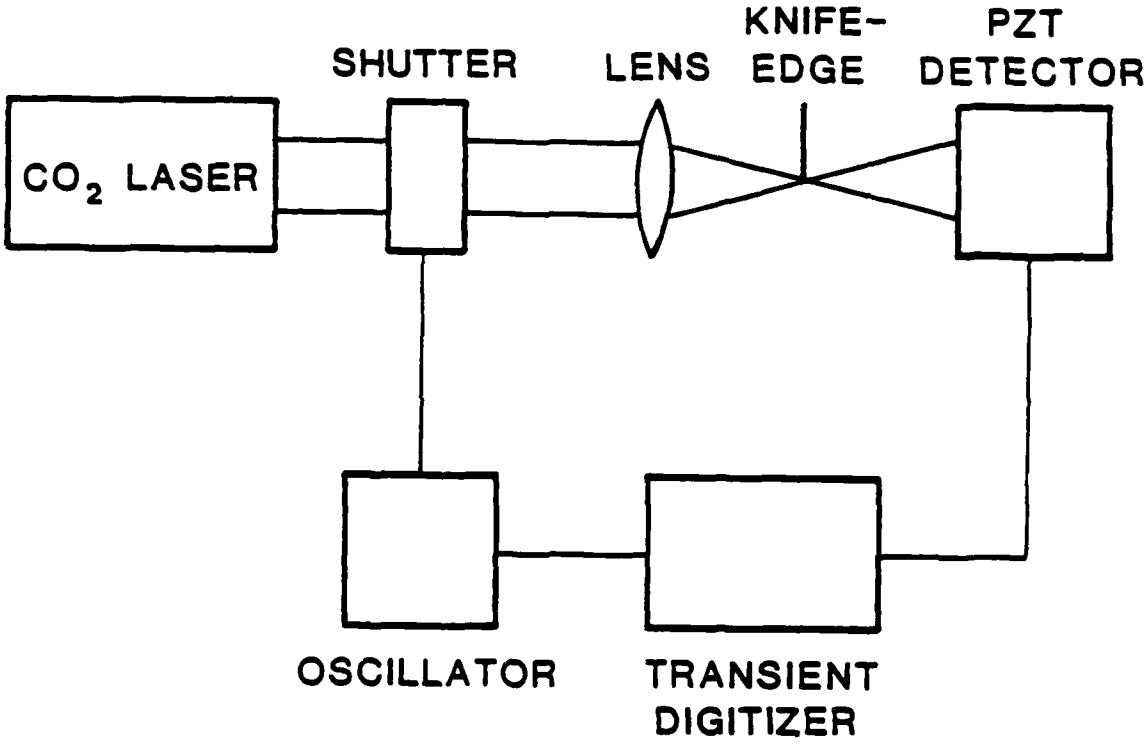
KNIFE-
EDGE
PZT
DETECTOR
SHUTTER
LENS
CO_2 LASER
OSCILLATOR
TRANSIENT
DIGITIZER

Fig. 5

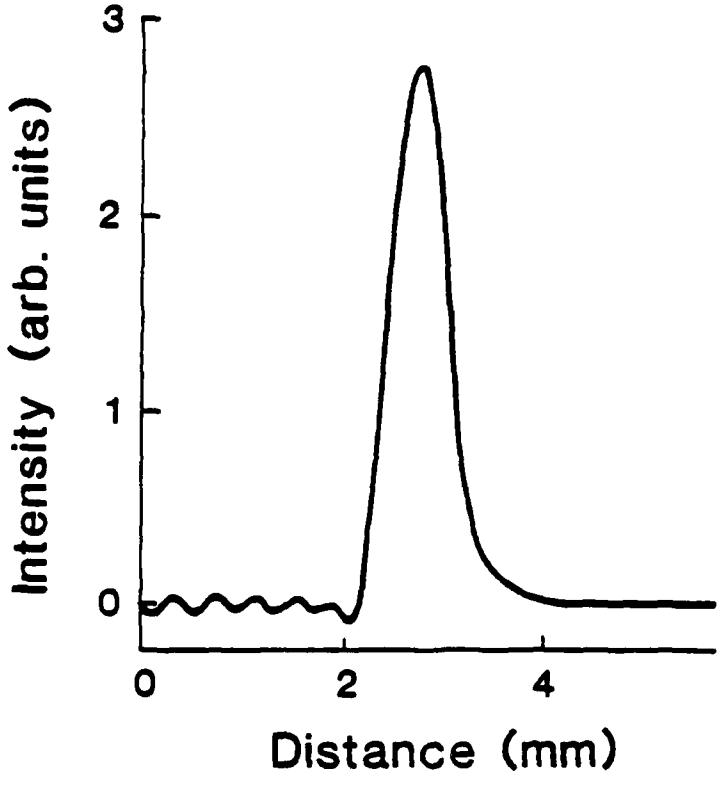

Fig 6

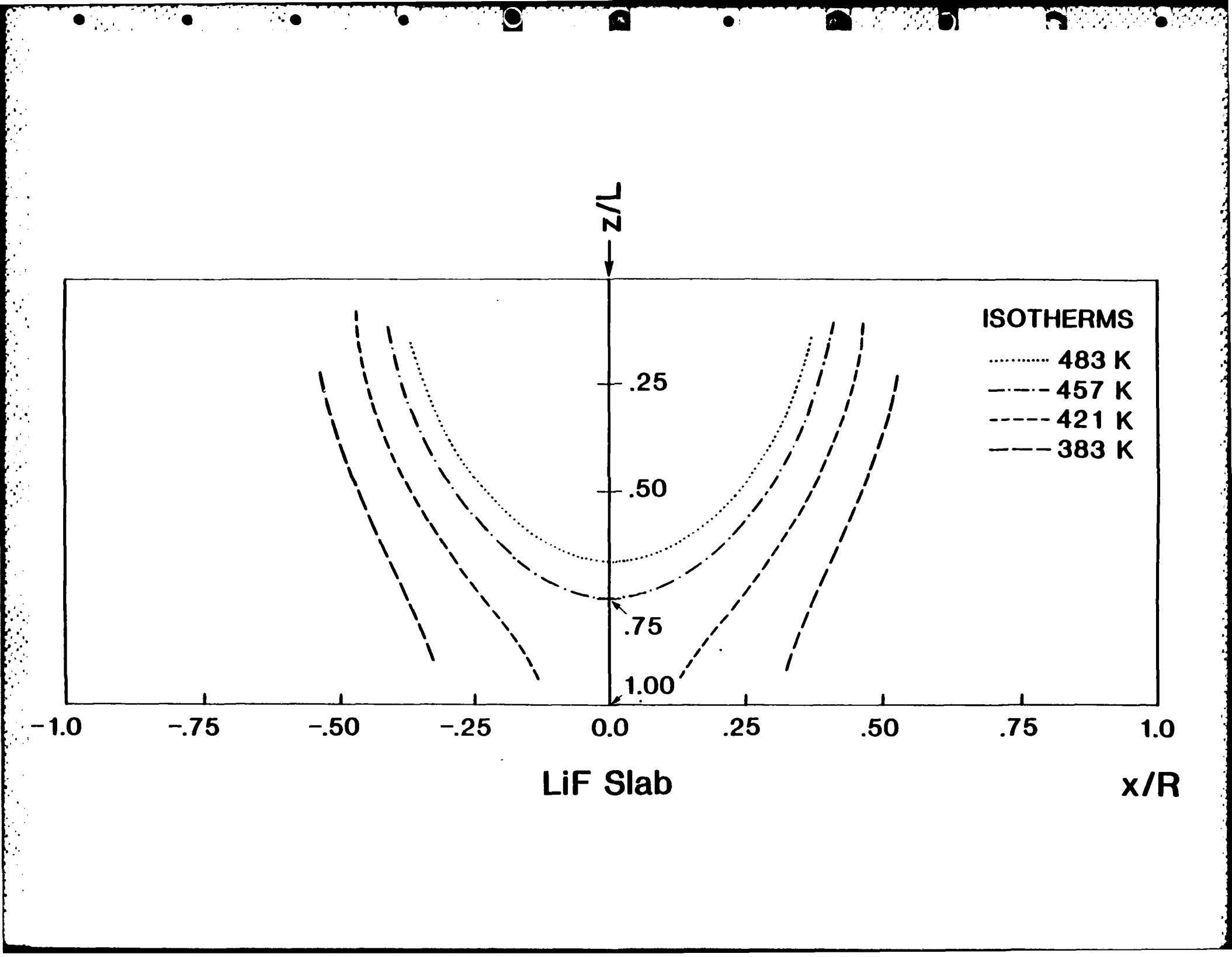
z/L
.25
.50
.75
1.00
ISOTHERMS
483 K
457 K
421 K
383 K
-1.0
-.75
-.50
-.25
0.0
.25
.50
.75
1.0
LiF Slab
x/R

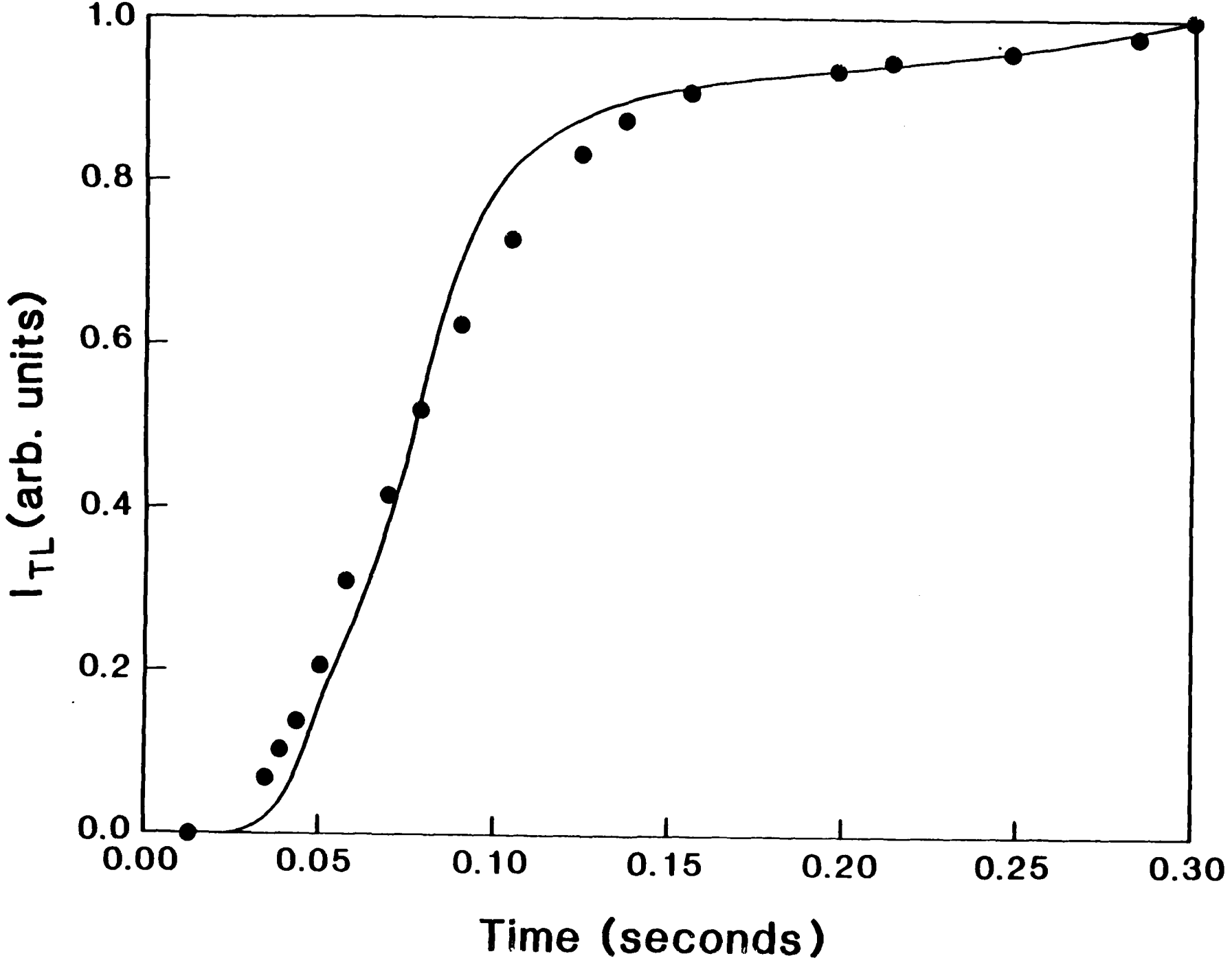
1.0
0.8
0.6
0.4
0.2
0.0
I_{TL} (arb. units)
0.00
0.05
0.10
0.15
0.20
0.25
0.30
Time (seconds)

Fig 9

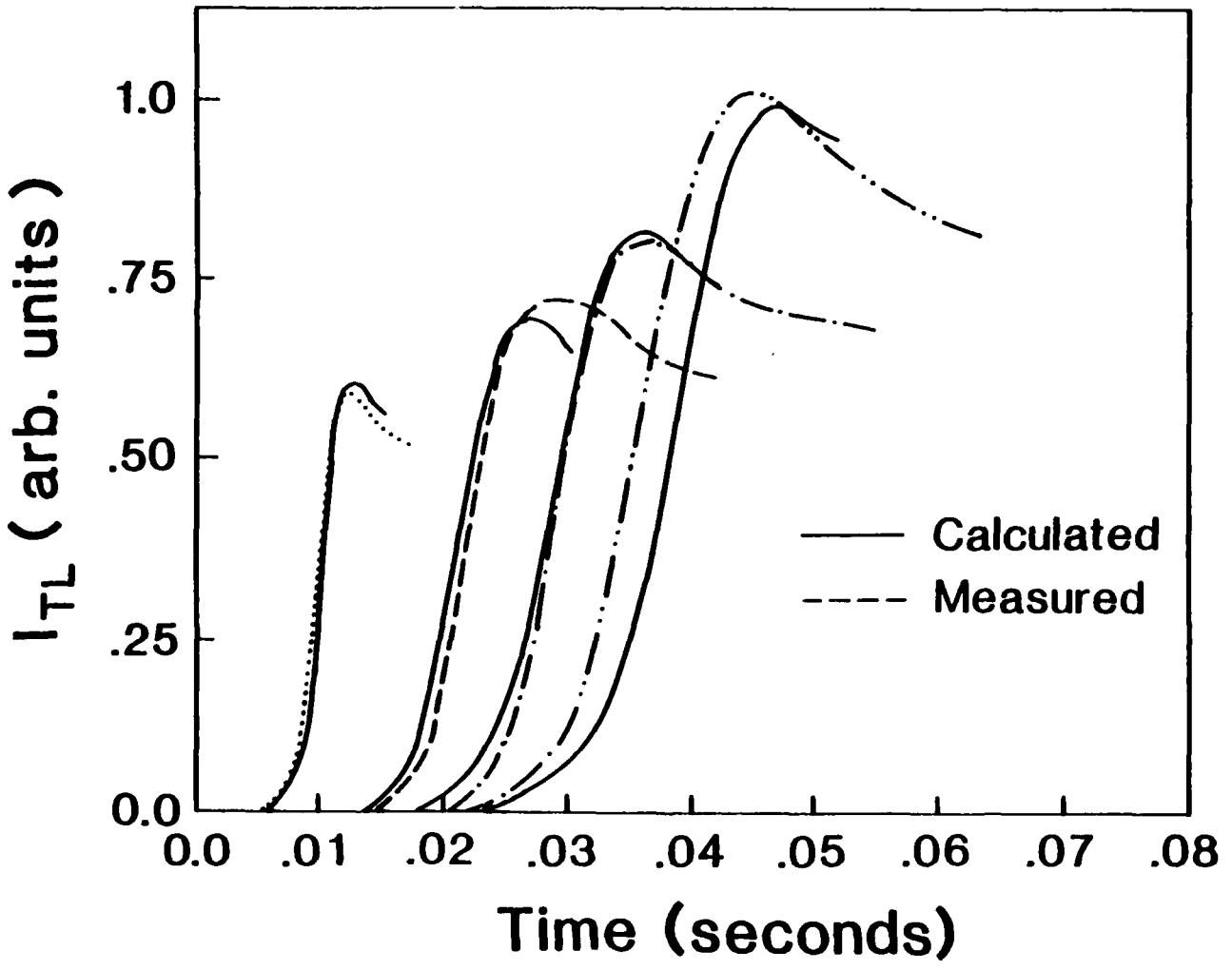
1.0
.75
.50
.25
0.0
I_{TL} (arb. units)
0.0
.01
.02
.03
.04
.05
.06
.07
.08
Time (seconds)
Calculated
Measured

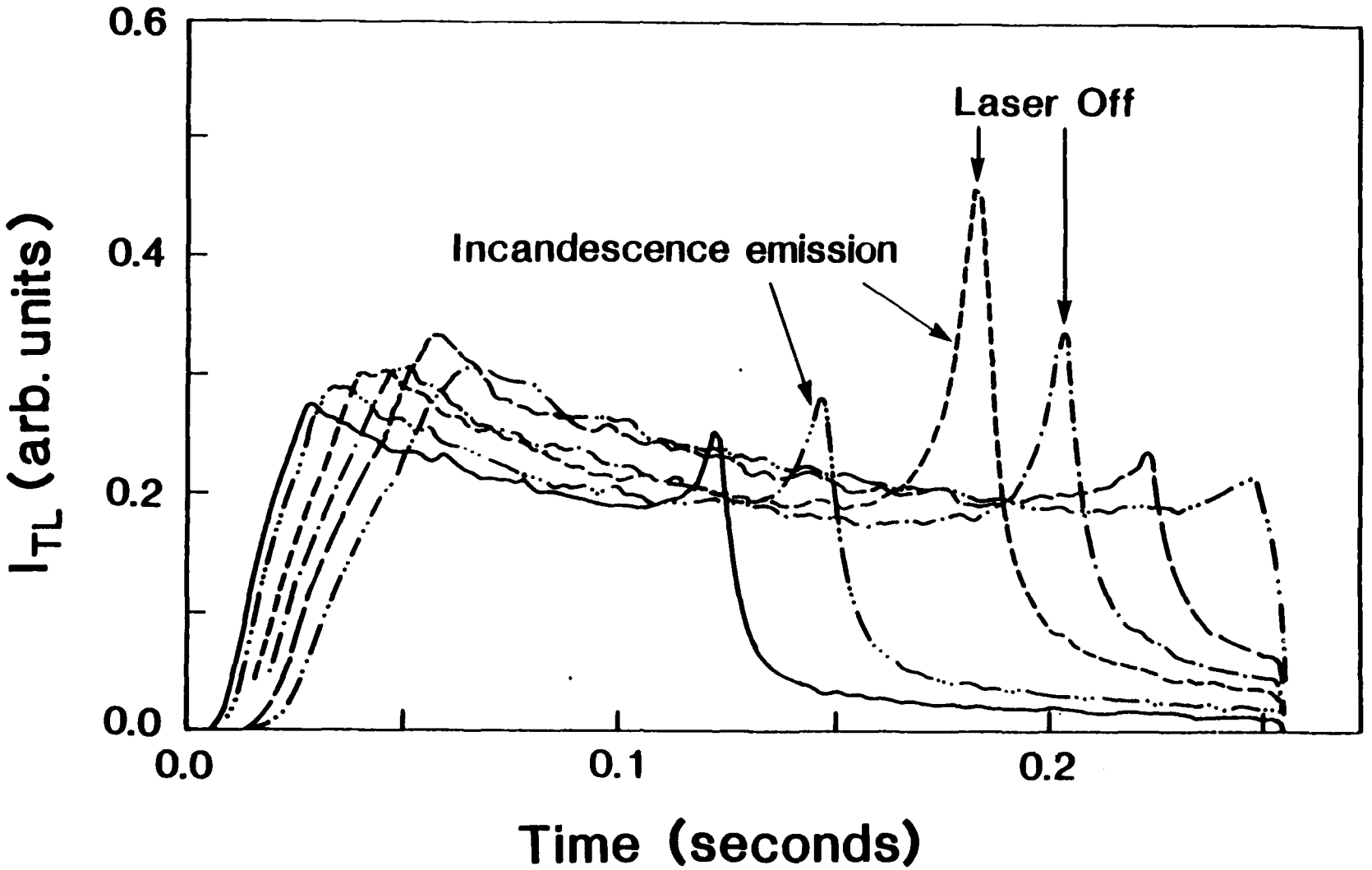
0.6
0.4
0.2
0.0
0.0
0.1
0.2
Laser Off
Incandescence emission
I_{TL} (arb. units)
Time (seconds)

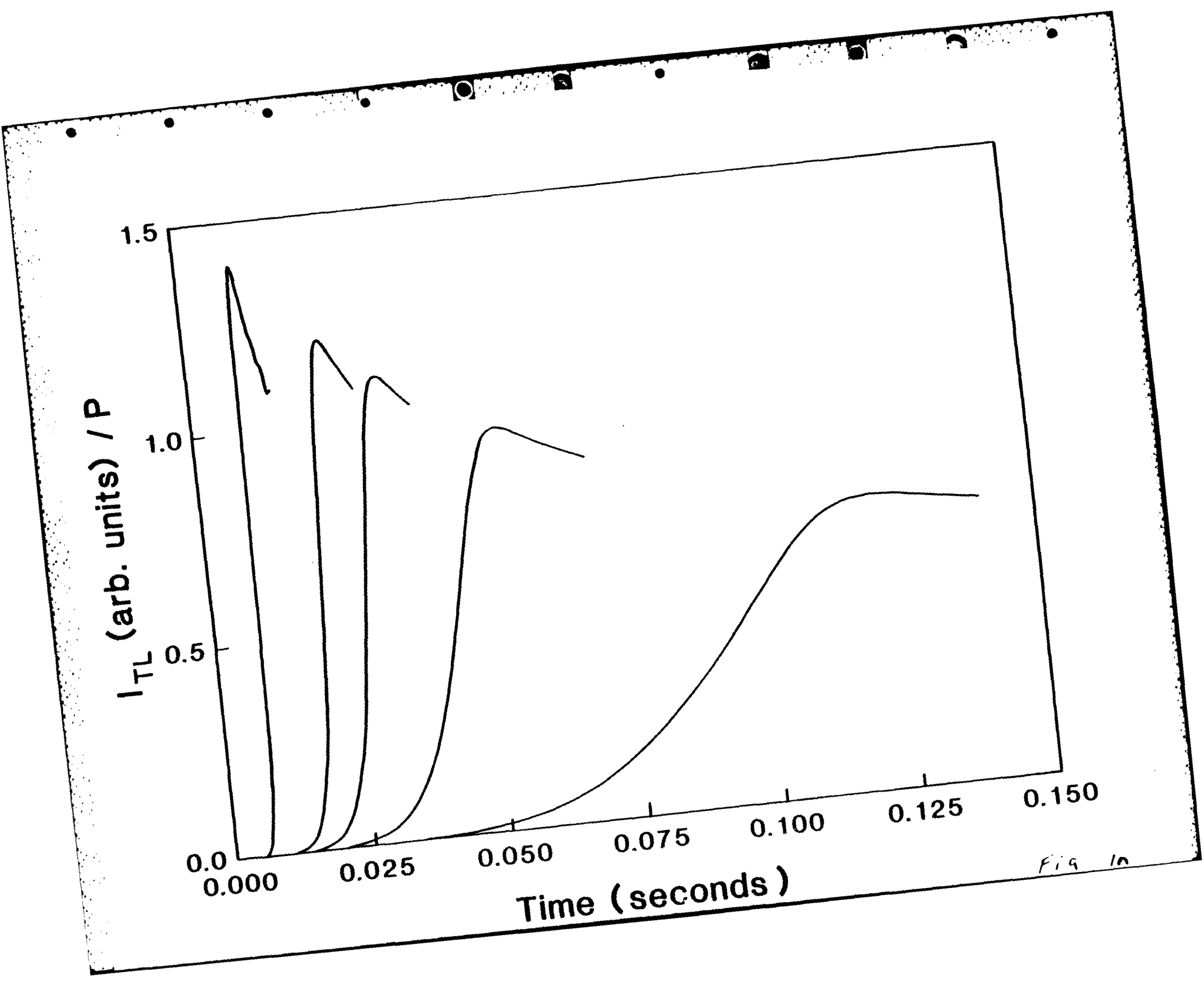
1.5
1.0
0.5
0.0
I_{TL} (arb. units) / P
0.000
0.025
0.050
0.075
0.100
0.125
0.150
Time (seconds)

Fig 10

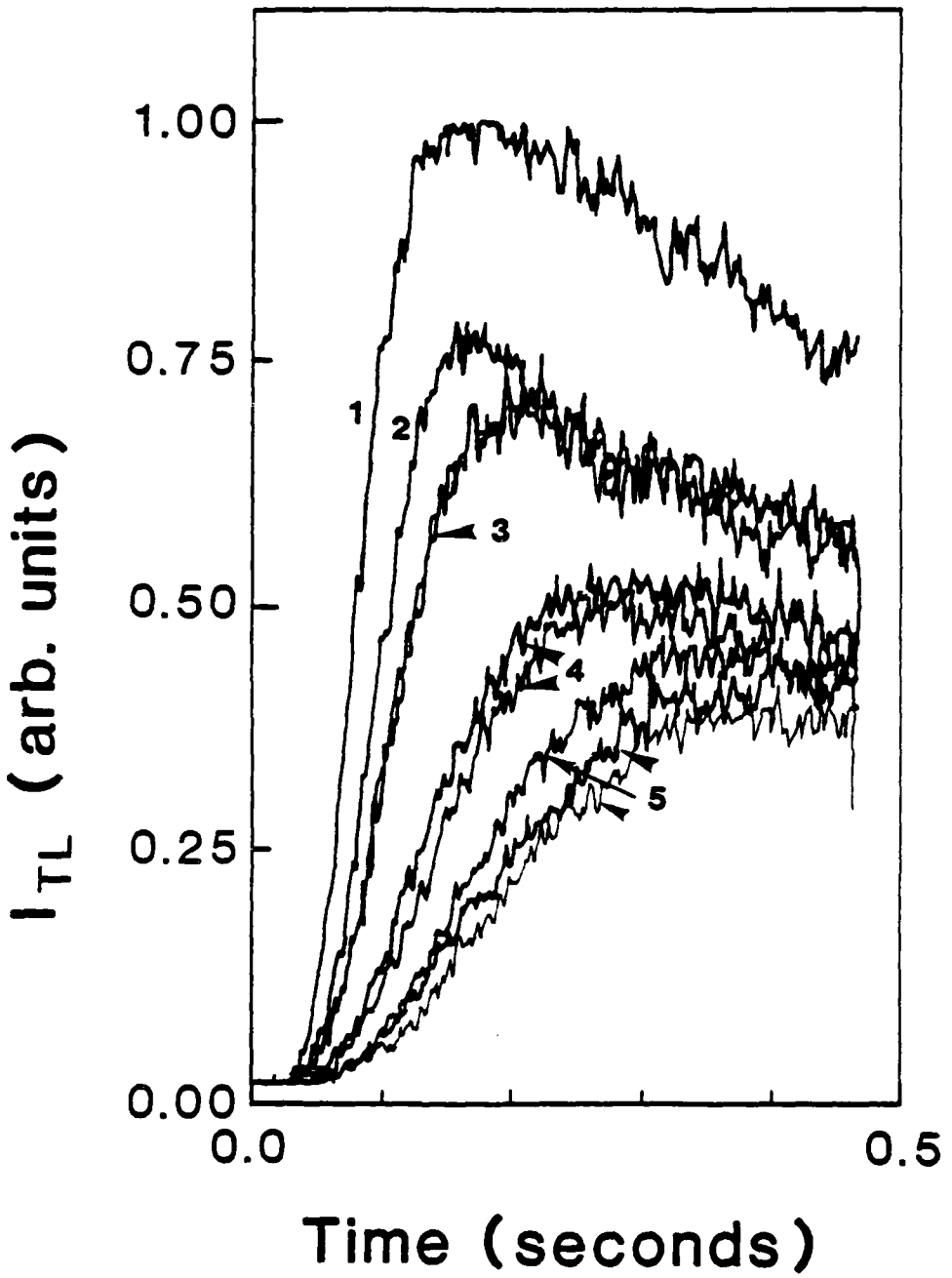

Fig. 12

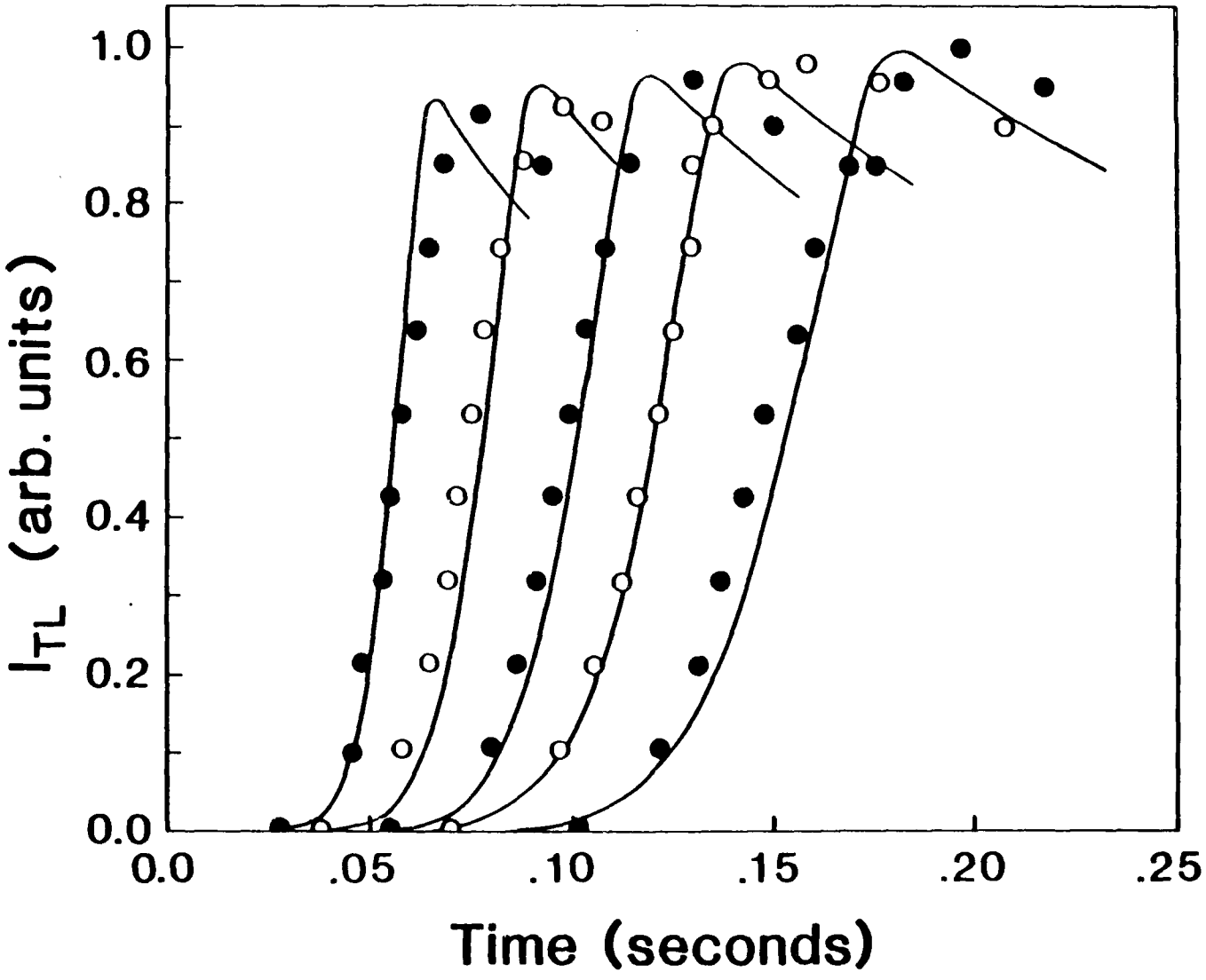
1.0
0.8
0.6
0.4
0.2
0.0
I_{TL} (arb. units)
0.0
.05
.10
.15
.20
.25
Time (seconds)

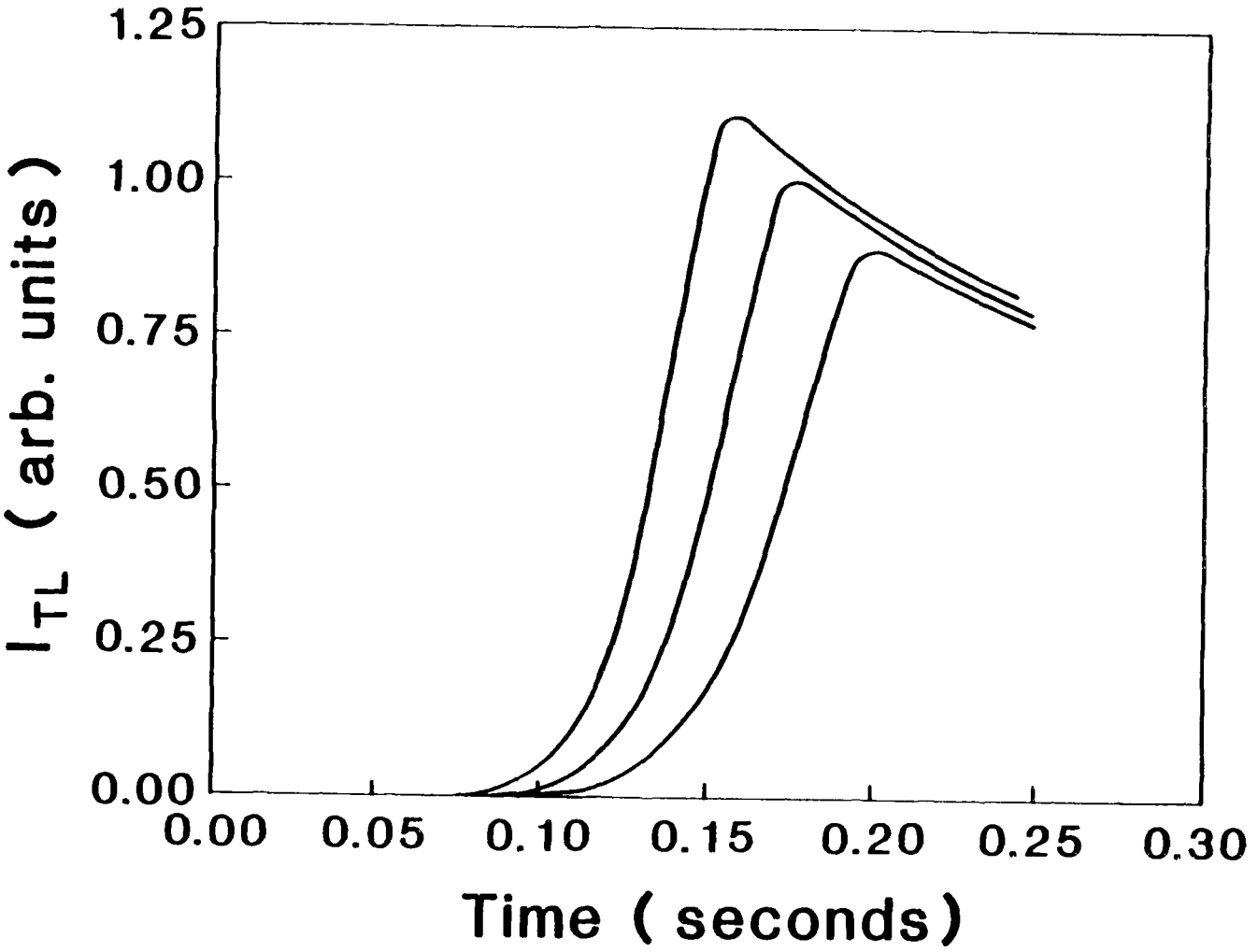
1.25
1.00
0.75
0.50
0.25
0.00
I_{TL} (arb. units)
0.00
0.05
0.10
0.15
0.20
0.25
0.30
Time (seconds)

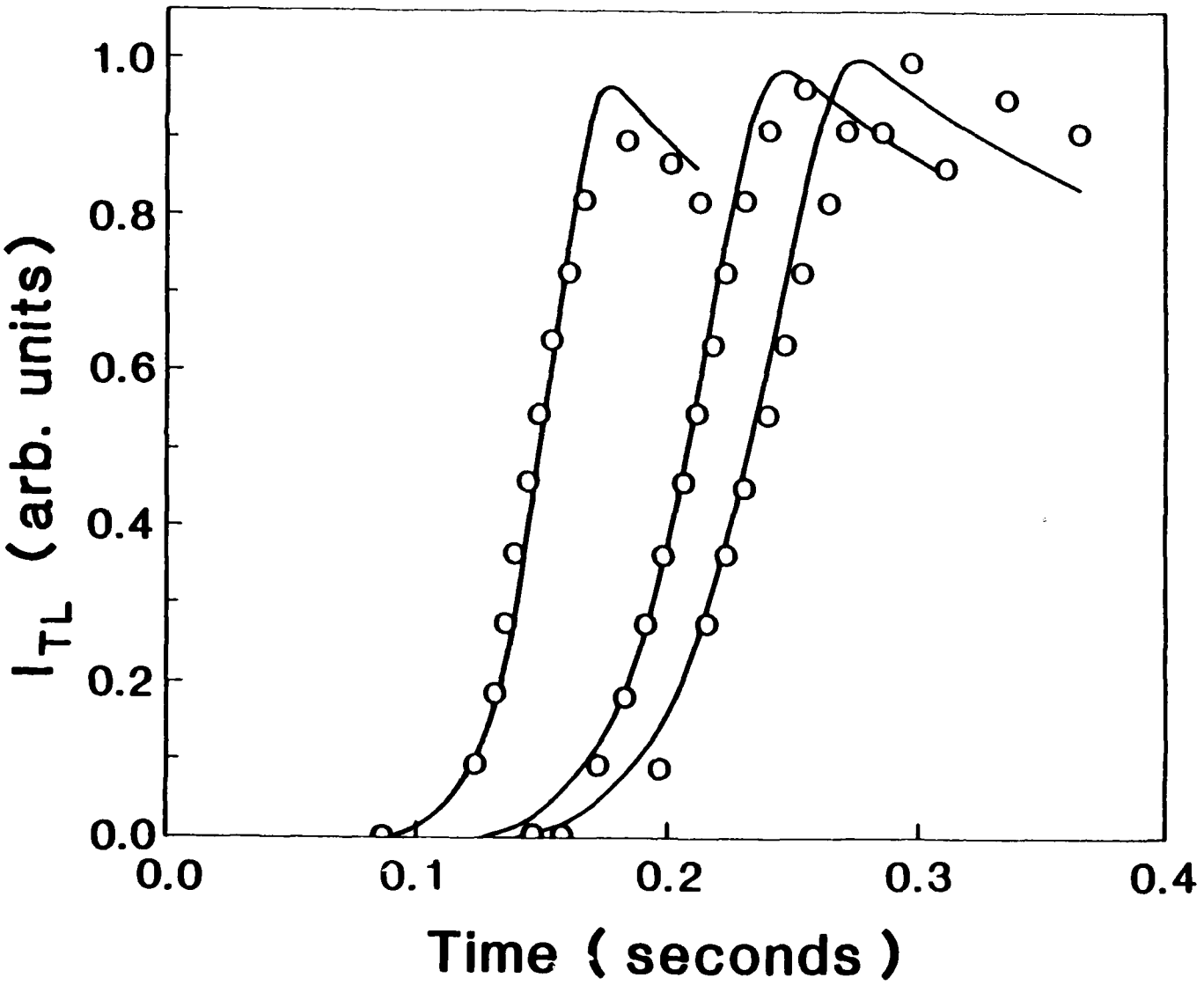
1.0
0.8
0.6
0.4
0.2
0.0
I_{TL} (arb. units)
0.0
0.1
0.2
0.3
0.4
Time (seconds)

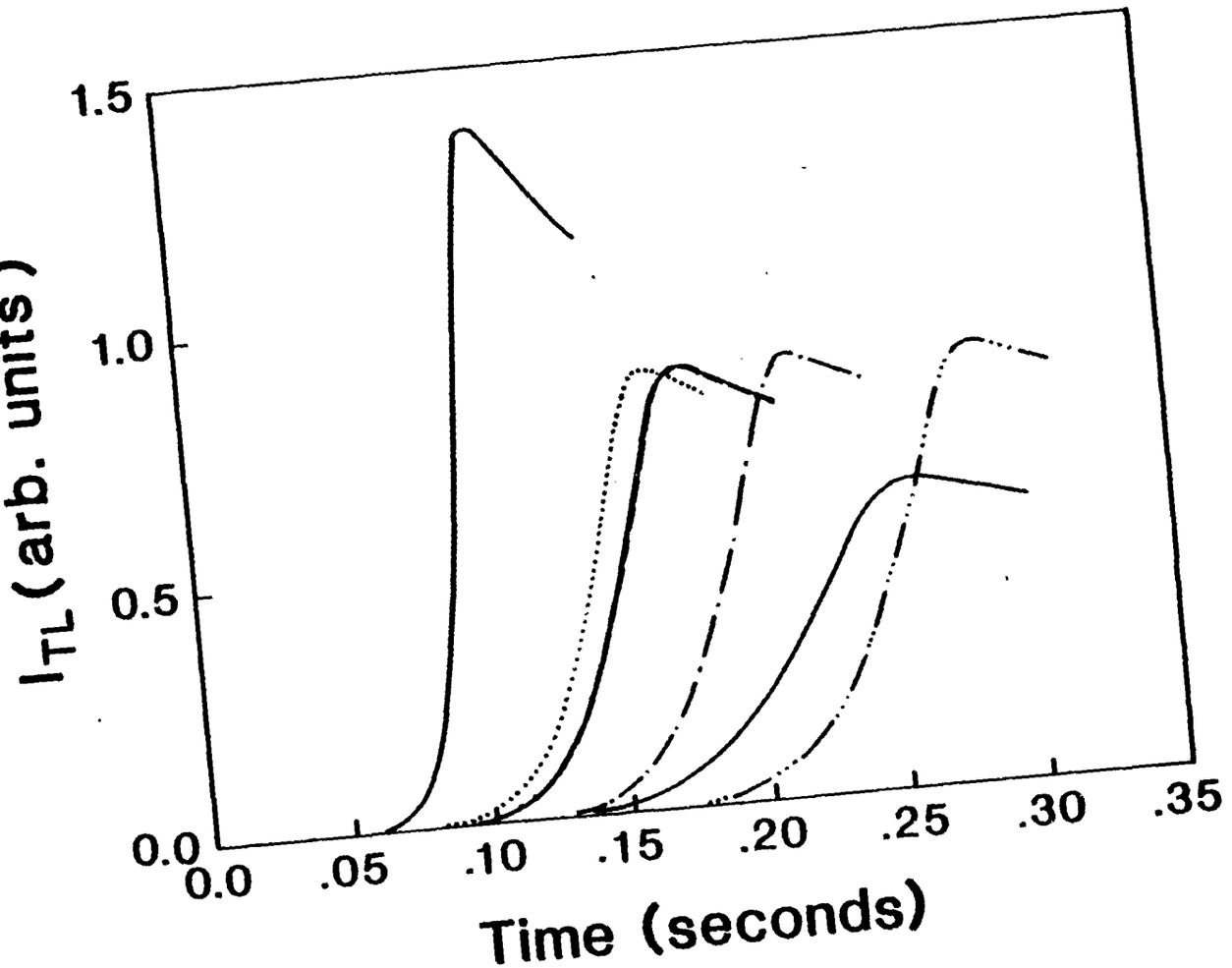
1.5
1.0
0.5
0.0
I_{TL} (arb. units)
0.0
.05
.10
.15
.20
.25
.30
.35
Time (seconds)

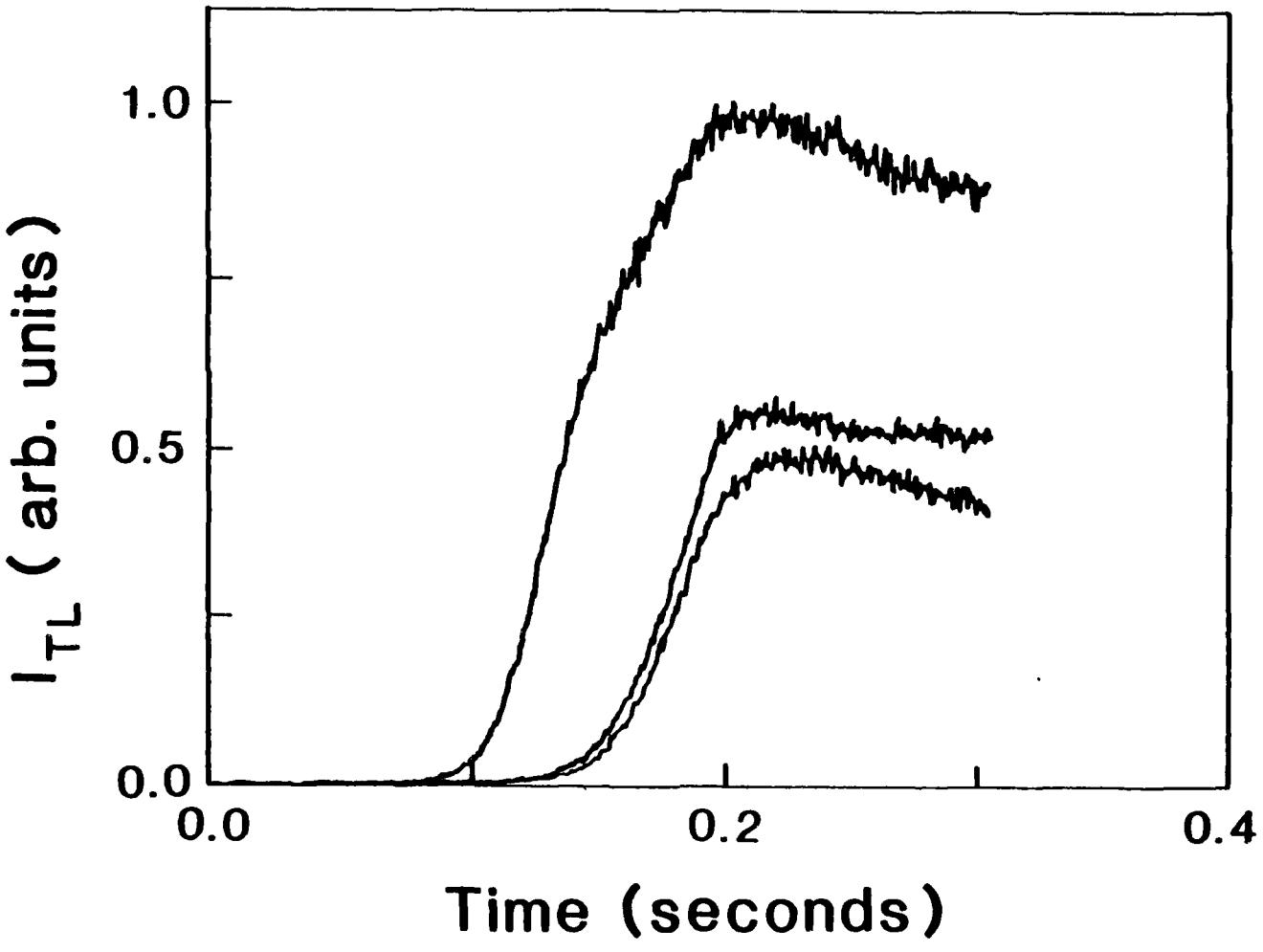

Fig 15

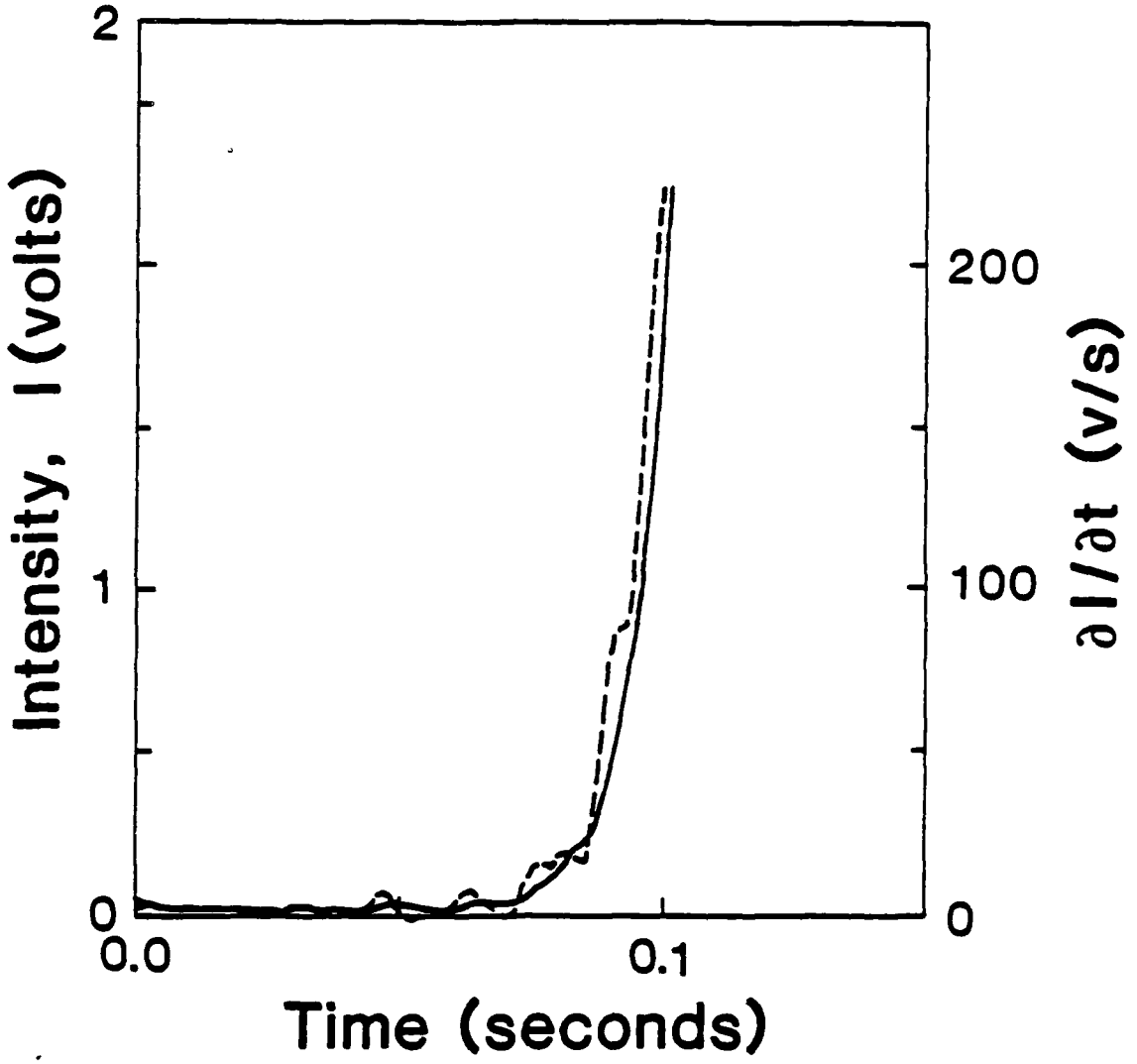

Fig. 16

APPENDIX C

AN ADVANCED RESEARCH FACILITY FOR LASER HEATING IN THERMOLUMINESCENCE

After completion of the research on the heat transfer from a Gaussian laser beam to semi-infinite thin-layer dosimeter configurations and of the resulting thermoluminescence response curves, a new apparatus was designed. This facility is needed to study these aspects in a situation that closely resembles the experimental conditions which have evolved as the ones that most likely will exist in actual field use of laser-heated thermoluminescnece dosimetry readers to be developed in the next two years.

These conditions are the following:

a. The laser beam must have a uniform intensity profile, be highly stable, reproducible, and computer-controllable.

b. The laser power must be at least 40 Watts.

c. For maximum sensitivity of the dose measurements, the spot size should be at least 3x3 mm^2. The high laser power is needed to heat this spot in less than 200 ms to 400 deg. C.

d. Since the beam optics exhibits a polarization dependence of the reflectivity, it is mandatory to assure that the beam polarization remains fixed during operation of the system.

The new system that was constructed and is presently being tested features a 40 Watt RF excited CO laser emitting a one cm diameter "halo" beam (doughnut-shaped cross section) of fixed polarization (Model L35PS, Directed Energy, Inc., Irvine, California). The polarization stability is achieved by an intra-cavity ZnSe polarizer plate that is mounted inside the beryllia discharge tube. The uniform beam profile is obtained by tightly focussing this beam with a short focal length Ge lens into a gold-coated optical channel of 3x3 mm^2 cross section. The optical layout is schematically shown in Fig.17.

A ZnSe beamsplitter is placed immediately after the focussing cube (shown as a concave mirror in Fig.17), and its position is adjusted so as to direct the small reflected beam to the center of the PZT detector. The chopping wheel, turning at 2000 rpm, has three 1 mm wide slots that permit the beam to hit the detector once every 10 ms. The PZT detector has a 5x5 mm^2 sensitive area. The pulsed signal it generates is used as the input signal for the laser control electronics described below.

A nitrogen purge inlet is located just below the small Ge lens at the top of the optical channel, and the nitrogen flows down onto the dosemeter and into the dosemeter reading chamber. The dosemeter is positioned at the exit of and very close to the optical channel. A light guide transmits the emitted luminescence to the photomultiplier tube (PMT).

The Control Electronics:

When a dosimeter read cycle is initiated, the following operation sequence is performed by the control electronics

1. The laser is turned on and the laser power is measured and adjusted until the laser is stabilized at the desired polarization and power level. This typically requires 100 to 300 ms. During this time the shutter remains closed and the dosemeter is not exposed to the laser beam

2. When the desired laser power is obtained, the shutter is opened for the desired heating time. It is possible that the laser power and/or the polarization may suddenly change during the time that the dosemeter is heated. If this occurs, indicators on the front panel of the control electronics are set to indicate the occurrence of this condition. A trigger output provides an output pulse corresponding to the heating cycle

3. At the conclusion of the heating cycle the shutter is closed and the laser is turned off. The system is immediately ready to begin another read cycle.

Laser power control is accomplished by pulse width modulation of the 30 kHz laser modulation signal. The laser power control function will normally maintain the measured power within less than 1% of the laser power setpoint. However, a sudden change in the laser polarization or output power may result in a deviation of more than 1%. To check for the occurrence of this condition, a power checking circuit is used to check for a power error of greater than 3%. The dosemeter read cycle is inhibited when this condition occurs. If a dosemeter read cycle has already been started, an indicator is set to warn of the power error.

In addition to the power checking, there is another checking circuit that is used to avoid the use of the laser when undesirable polarization is present. Should the beam polarization deviate from the desired polarization, the beamsplitter reflects a greater or smaller percentage of the incident power. This gives an erroneous indication of increased laser power. This condition can be detected because it results in a substantial change in the control voltage. For a given laser power setpoint, an acceptable range in control voltage can be determined, and these limits are then used to check for this polarization change. This checking function is referred to as control voltage checking. A dosemeter read cycle is inhibited when this condition is present, and a control error indicator is set if this condition occurs after a dosemeter read cycle has been started.

The addition of a temperature stabilized base for the present laser head (Neslab refrigerated recirculating heat exchanger model RTE-5DD) further assures stable operation of the laser as it maintains the laser discharge tube at a constant temperature ($\pm$.1 deg. C).

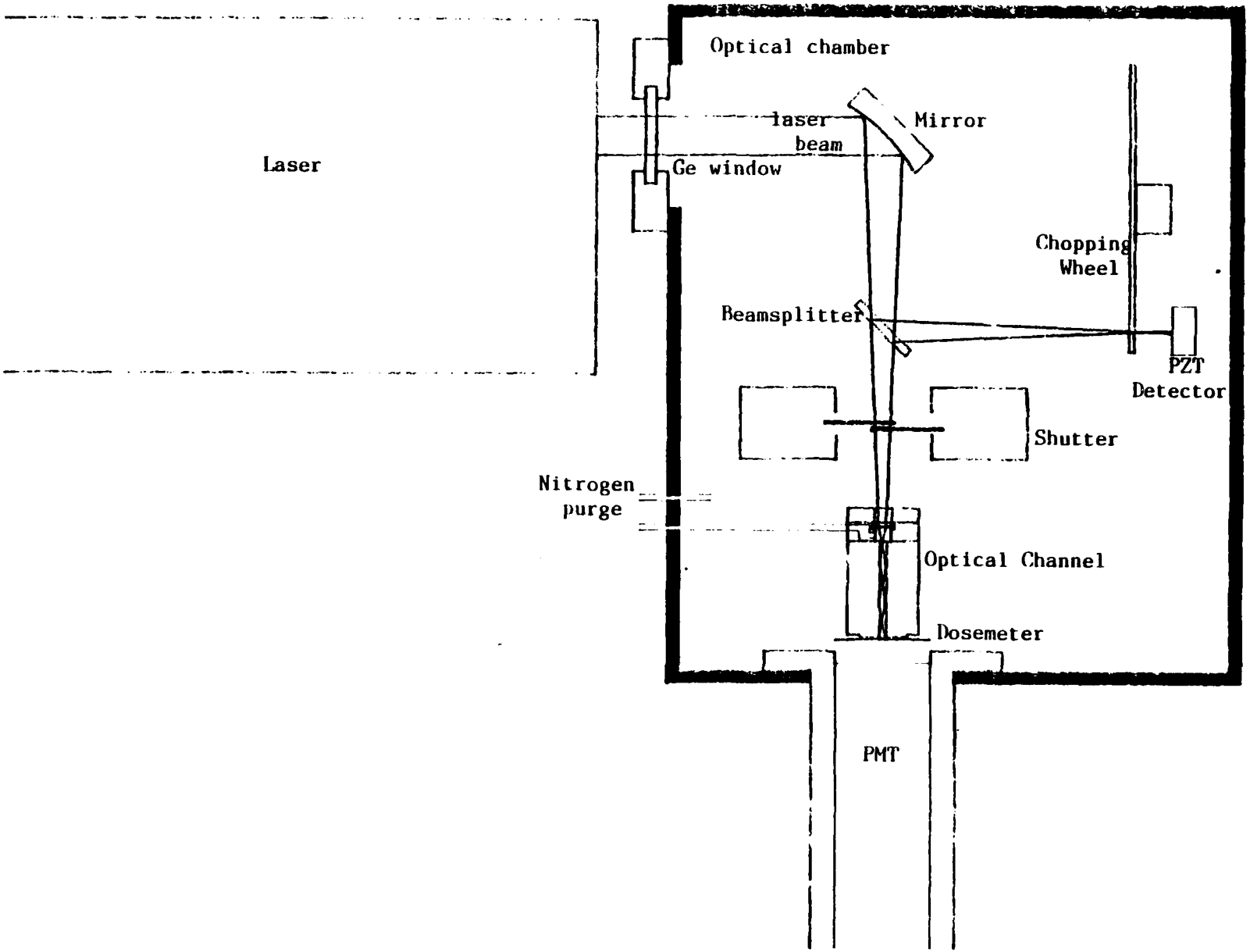

Fig. 17: Optics of the Proposed Laser TLD Reader (Vertical layout)

OFFICE OF NAVAL RESEARCH

PUBLICATIONS / PATENTS / PRESENTATIONS / HONORS REPORT

for

1 October 1983 through 31 March, 1985

for

Contract N00014-82-K-0529

Project-Task Area No. RR011-07-01

Work Unit No. NR395-079

INVESTIGATION OF BASIC CHARACTERISTICS OF LASER HEATING IN THERMOLUMINESCENCE

Principle Investigator: Peter F. Braunlich

WASHINGTON STATE UNIVERSITY
DEPARTMENT OF PHYSICS
PULLMAN, WA 99164-2814

INVITED PRESENTATIONS AT TOPICAL OR SCIENTIFIC/TECHNICAL CONFERENCES:

"LASER HEATING TECHNIQUES IN BETA THERMOLUMIENSCENCE DOSIMETRY"

by

P. Braunlich and W. Tetzlaff

INVITED PRESENTATION

29TH ANNUAL MEETING OF THE AMERICAN HEALTH PHYSICS SOCIETY

JUNE 3 - 7, 1984

NEW ORLEANS, USA

HONORS/AWARDS: NONE

BOOKS: NONE

PATENTS FILED: NONE

PATENTS GRANTED: NONE

PAPERS PUBLISHED IN REFEREED JOURNALS:

1."THERMOLUMINESCENCE KINETICS AT THE EXTREME HEATING RATES POSSIBLE WITH LASER STIMULATION"
RADIATION PROTECTION DOSIMETRY VOL.6, PP. 25-28 (1984)

2."HEATING CONTINUOUS THERMOLUMINESCENT LAYERS WITH LOCALISED LASER BEAMS"
RADIATION PROTECTION DOSIMETRY VOL. 6, PP. 83-86 (1984)

3."THERMOLUMINESCENCE FAST NEUTRON DOSIMETRY BY LASER HEATING"
RADIATION PROTECTION DOSIMETRY VOL. 6, PP. 163-165 (1984)

PAPERS SUBMITTED TO REFEREED JOURNALS:

"LASER-STIMULATED THERMOLUMINESCENCE"

by

A. Abtahi, P. Braunlich, P. Kelly, and J. Gasiot

(Submitted to J. Appl. Physics on January 2, 1985)

REPORTS DISTRIBUTION LIST FOR ONR PHYSICS DIVISION OFFICE
UNCLASSIFIED CONTRACTS

Director Defense Advanced Research Projects Agency Attn: Technical Library 1400 Wilson Blvd. Arlington, Virginia 22209	1 copy
Office of Naval Research Physics Division Office (Code 412) 800 North Quincy Street Arlington, Virginia 22217	2 copies
Office of Naval Research Director, Technology (Code 200) 800 North Quincy Street Arlington, Virginia 22217	1 copy
Naval Research Laboratory Department of the Navy Attn: Technical Library Washington, DC 20375	1 copy
Office of the Director of Defense Research and Engineering Information Office Library Branch The Pentagon Washington, DC 20301	1 copy
U.S. Army Research Office Box 1211 Research Triangle Park North Carolina 27709	2 copies
Defense Technical Information Center Cameron Station Alexandria, Virginia 22314	12 copies
Director, National Bureau of Standards Attn: Technical Library Washington, DC 20234	1 copy
Director U.S. Army Engineering Research and Development Laboratories Attn: Technical Documents Center Fort Belvoir, Virginia 22060	1 copy
ODDR&E Advisory Group on Electron Devices 201 Varick Street New York, New York 10014	1 copy

Air Force Office of Scientific Research — 1 copy
Department of the Air Force
Bolling AFB, DC 22209

Air Force Weapons Laboratory — 1 copy
Technical Library
Kirtland Air Force Base
Albuquerque, New Mexico 87117

Air Force Avionics Laboratory — 1 copy
Air Force Systems Command
Technical Library
Wright-Patterson Air Force Base
Dayton, Ohio 45433

Lawrence Livermore Laboratory — 1 copy
Attn: Dr. W. F. Krupke
University of California
P.O. Box 808
Livermore, California 94550

Harry Diamond Laboratories — 1 copy
Technical Library
2800 Powder Mill Road
Adelphi, Maryland 20783

Naval Air Development Center — 1 copy
Attn: Technical Library
Johnsville
Warminster, Pennsylvania 18974

Naval Weapons Center — 1 copy
Technical Library (Code 753)
China Lake, California 93555

Naval Underwater Systems Center — 1 copy
Technical Center
New London, Connecticut 06320

Commandant of the Marine Corps — 1 copy
Scientific Advisor (Code RD-1)
Washington, DC 20380

Naval Ordnance Station — 1 copy
Technical Library
Indian Head, Maryland 20640

Naval Postgraduate School — 1 copy
Technical Library (Code 0212)
Monterey, California 93940

Naval Missile Center — 1 copy
Technical Library (Code 5632.2)
Point Mugu, California 93010

Naval Ordnance Station — 1 copy
Technical Library
Louisville, Kentucky 40214

Commanding Officer — 1 copy
Naval Ocean Research & Development Activity
Technical Library
NSTL Station, Mississippi 39529

Naval Explosive Ordnance Disposal Facility — 1 copy
Technical Library
Indian Head, Maryland 20640

Naval Ocean Systems Center — 1 copy
Technical Library
San Diego, California 92152

Naval Surface Weapons Center — 1 copy
Technical Library
Silver Spring, Maryland 20910

Naval Ship Research and Development Center — 1 copy
Central Library (Code L42 and L43)
Bethesda, Maryland 20084

Naval Avionics Facility — 1 copy
Technical Library
Indianapolis, Indiana 46218

END

FILMED

5-85

DTIC